CHEMICAL REVIEWS

Review

pubs.acs.org/CR

Nucleic Acid Catalysis: Metals, Nucleobases, and Other Cofactors

W. Luke Ward,[†,‡,§] Kory Plakos,[†,‡] and Victoria J. DeRose*[,†]

[†]Department of Chemistry and Biochemistry and [‡]Institute of Molecular Biology, University of Oregon, Eugene, Oregon 97403, United States

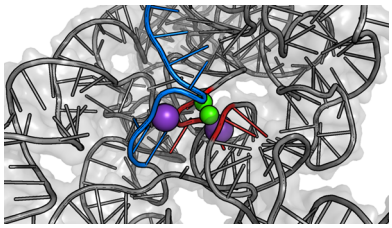

CONTENTS

1. INTRODUCTION AND SCOPE OF THIS REVIEW

The discovery of RNA-catalyzed phosphodiester bond cleavage by Cech and Altman in 1982–1983 shattered the paradigm of protein-dependent biological catalysis and opened up new horizons for RNA biology (reviewed in ref 1). These discoveries ushered in a new era of high activity in RNA biochemistry and structural biology that, in conjunction with developments in genomics, established groundwork for the ensuing explosion in discoveries of other functional but noncoding RNAs. Since the initial discoveries, several classes of naturally occurring and artificially developed ribozymes have been defined. Ribozyme reactions catalyzed in nature include phosphoryl and aminoacyl transfer reactions (Figure 1). RNA-catalyzed reactions obtained in vitro extend to carbon–carbon bond formation in the Diels–Alderase ribozyme. In vitro selection has also been employed to discover DNA-based enzymes that catalyze a number of different reactions, including RNA cleavage, as in Figure 1A.

As with metalloproteins, the active sites of several ribozymes include site-specific metal-ion cofactors whose properties influence chemical reactivity. The bioinorganic chemistry of

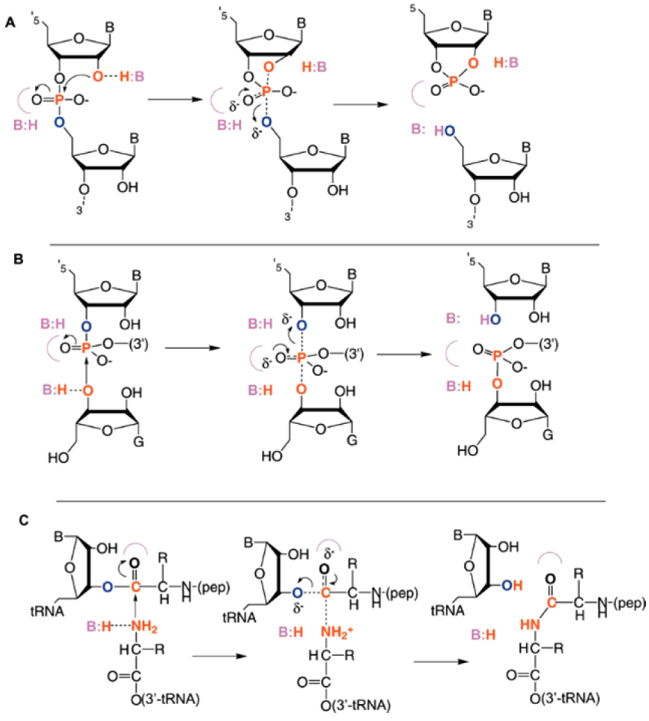

Figure 1. Reactions catalyzed by naturally occurring ribozymes. (A) Intramolecular phosphoryl-transfer reaction catalyzed by the "nucleolytic" ribozymes including the hammerhead, hepatitis delta virus (HDV), hairpin, *Neurospora* VS, and GlmS RNAs. (B) Group I and group II introns catalyze attack of an extrinsic nucleophile, here shown as a guanosine, at a specific phosphodiester bond. (C) Peptidyl transfer catalyzed in the active site of the ribosome. Reprinted with permission from ref 2. Copyright 2002 Elsevier Science, Ltd.

Special Issue: 2014 Bioinorganic Enzymology

Received: August 30, 2013
Published: April 14, 2014

   dx.doi.org/10.1021/cr400476k | *Chem. Rev.* 2014, 114, 4318–4342

RNA differs significantly from that of proteins, however. Unlike metalloproteins, the naturally occurring ribozymes discovered (so far) do not catalyze redox reactions. Based on cell availability and in vitro activity reconstitution, the cation cofactors for ribozymes are presumed to be Mg^{2+}, with occasional evidence for localized monovalent K^+ ions. It should be noted that transition metals certainly bind to RNAs and might have regulatory[3] or early biotic[4] roles, and in some cases, they can support high activity in ribozymes, but evidence for transition-metal-supported ribozyme activity in vivo is not established. In addition, unlike in the case of most proteins, the influence of inorganic cations on RNA structure, particularly tertiary structure, is very strong. RNA is a negatively charged biopolymer, carrying one charge per phosphodiester bond. The four nucleobases are expected to be neutral except in rare cases. Thus, as a negatively charged polyelectrolyte, RNA carries an "atmosphere" of neutralizing cations, and cation concentration and identity can critically influence global and local structure. A major challenge for mechanistic and structural studies in ribozymes has been separating the influence of metal-ion cofactors on structure from their influence on chemical reactivity.

Since the discovery of ribozymes, the central quest has been to understand how the relatively limited chemical functionalities of oligonucleotides are able to catalyze reactions with nearly the same efficiency and selectivity as proteins. Because of the dearth of diverse functional groups (specifically cationic) and because most RNAs fold more efficiently with addition of Mg^{2+}, in early days, there was a strong focus on the potential for ribozymes to be Mg^{2+}-dependent metalloenzymes.[5,6] As structure–function studies have advanced, focus has also turned to the potential for RNA nucleobases to participate in catalysis,[7] as well as the synergy between active-site nucleobase and metal-ion contributions.[8,9]

The main focus of this review is metal-ion-assisted catalysis in ribozyme mechanisms. Two classes of phosphoryl-transfer-catalyzing ribozymes are discussed in this review. Class I ribozymes catalyze the attack of a specific phosphodiester bond by an exogenous nucleophile, resulting in strand scission with a 3′- or 5′-oxygen leaving group. The exogenous nucleophile can be water or an RNA 2′-OH group, resulting also in a new phosphodiester bond (Figure 1B). Class II ribozymes catalyze the attack of a 2′-OH group on its own 3′-phosphodiester center, resulting in strand scission with a 5′-OH leaving group and a 2′,3′-cyclic phosphate (Figure 1A). Within the ribosome, transfer of an amino acid from the 3′-end of aminoacylated tRNA results in formation of a new peptide bond (Figure 1C). We do not review the active site of the ribosome. Although the ribosome-catalyzed reaction is clearly an RNA-dependent reaction governed by an intricate RNA active site, specific roles for metal ions are not evident in this reaction, and it has been recently reviewed.[11] We do discuss, albeit more briefly, the hairpin and Diels–Alderase ribozymes. Neither of these ribozymes have specific metal-ion cofactors, but their active sites provide demonstrations of the other roles contributed by RNA moieties in catalyzing reactions. Like RNA, DNA can adopt complex structures, and DNA-based catalysts have been derived that depend on and, in some cases, sense metal ions. This topic is also briefly reviewed to acquaint the reader with that field. Included in this review is also a brief overview of methods applied to studies of ribozymes, as some aspects of this field differ from similar activities in protein enzymology.

Not included in this ribozyme review, but of interest to the bioinorganic chemistry of RNA, are the fascinating cases of "functional" metal-ion interactions in RNAs that do not perform chemical reactions but whose metal-dependent structure governs gene expression. These include metal-dependent riboswitches[3] that govern expression of Mg^{2+} transporters and the Fe-dependent iron-responsive element.[10] In both of these systems, metal-dependent conformational changes in RNA structure govern downstream expression of metal-uptake genes.

Several other reviews of ribozymes have appeared in the past 10 years.[8,12−14] Because cations are so important for RNA structure–function relationships, the topic of RNA–metal interactions has also been examined extensively outside the ribozyme field. Recent reviews on RNA–metal or RNA–ion-atmosphere interactions have focused on thermodynamics,[15] detection by biochemical,[16] spectroscopic,[17,18] or X-ray scattering[19] methods, and metal-coordination properties of nucleic acids.[9,20,21]

2. PROPERTIES OF RNA

Ribozymes, like other enzymes, use a variety of strategies to lower the energetic barriers of chemical reactions.[22] Perhaps the most ubiquitous of these strategies is the creation of an active site that binds reactive species and thereby provides substantial entropic gains. The active site can also position functional groups from the substrate, enzyme, solvent, and cofactors to assist catalysis. Electronic properties of functional groups, manifested as shifts in nucleophilicity or pK_a, might be tuned by the electrostatic environment of the active site. Typically, an active site is protected from bulk solvent. Together, these properties might act to destabilize a ground state and/or stabilize a transition or product state. Although these are common and well-studied strategies for proteinaceous enzymes, there are particularly challenging aspects about the nature of ribonucleic acids that ribozymes must overcome to efficiently organize an active site and catalyze chemical reactions.

2.1. Chemical Properties of RNA

The most obvious difference between RNA and proteins, and seemingly greatest challenge to RNA (and DNA) chemistry in general, is the lack of chemical diversity provided by the four standard nucleobases (Figure 2) in comparison with 20 common amino acids. Nucleobases afford amino and imino nitrogen groups with pK_a values above 9 or below 4, but not the near-neutral pK_a of the histidine imidazole. The keto oxygens of nucleobases provide hydrogen-bond donor groups and electrostatic tuning, but there are no carboxylic acids for proton shuttles or metal chelation. In RNA, negative charges occur only on phosphodiester nonbridging oxygen atoms with pK_a values of <1.5. Phosphodiesters can position groups through hydrogen bonding and coordinate "hard" metal ions, but unlike a glutamate or aspartate encoded within a protein sequence, the ubiquitous phosphodiester groups are difficult to uniquely position within an RNA structure.

Given these limitations, the fact that RNA sequences can encode enough structural diversity to create active sites, to selectively bind small molecules and cofactors, and to tune the properties of these groups for chemical reactivity is fairly amazing. One advantage is found in the varieties of secondary and tertiary elements, such as helices, loops, bulges, and base triples, that allow RNA to fold into complex structures that enable the formation of intricate active sites.[23] This complexity

dx.doi.org/10.1021/cr400476k | Chem. Rev. 2014, 114, 4318–4342

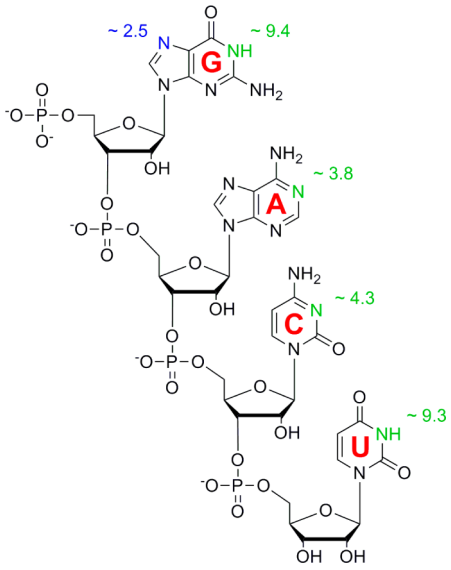

Figure 2. RNA oligonucleotide, with nucleobase solution pK_a values from ref 13.

is supported by networks of hydrogen bonds and is sometimes evidenced by the ability of single-atom substitutions to disrupt global folding.

2.2. Metals and RNA

Metal-ion interactions with RNA, a negatively charged polyelectrolyte, range from general charge shielding to highly specific coordination sites. Cations nonspecifically condense around the negative charge of the phosphodiester backbone, resulting in a mobile counterion atmosphere that provides general charge shielding. Although monovalent cations can fulfill this role, the charge density of divalent metals can add stability in regions where several phosphates come within close proximity, such as in RNA turns or helical junctions. RNAs also create specific sites for metal-ion association that are important to structure and function. Electron-rich groups (e.g., imino nitrogens, phosphate oxygens, and keto oxygens) are available to coordinate metal ions. In some cases, a metal ion can coordinate two or more groups from separate secondary structural motifs, thereby bridging domains and stabilizing a specific tertiary structure.[20] Multidentate interactions within a ribozyme active site may provide the additional stabilizing contacts needed to overcome strained conformations necessary for achieving optimal geometry of reactive groups.

In addition to providing ribozymes with structural stability, metal ions can play key roles in catalysis (Figure 3). A metal hydroxide can act as a general base to deprotonate a 2′-OH group, thereby activating the oxygen as a nucleophile as is predicted for RNase P and possibly for the hepatitis delta virus and hammerhead ribozymes (vide infra). Moreover, a bound metal could potentially organize a water molecule for general acid catalysis. Inner-sphere coordination might also play important roles in ribozymes. For instance, coordination by a metal to a phosphate oxygen in the ground state increases the electrophilicity of the phosphorus by withdrawing electron density. Further, coordination to a phosphate oxygen can stabilize the negative charge accumulation of the proposed trigonal-bipyramidal phosphorane transition state of phosphoryl-transfer reactions. Inner-sphere coordination to a 2′-OH group could aid in lowering its pK_a, enabling a base to abstract the proton. These types of active-site inner-sphere coordination modes are observed in the group I and group II introns and potentially in the hammerhead ribozyme (vide infra).

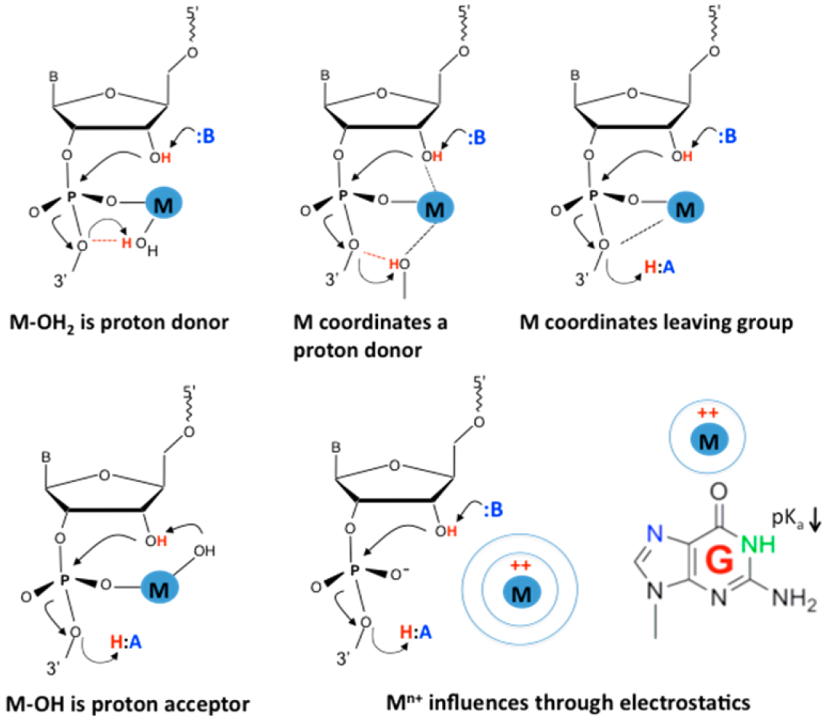

Figure 3. Potential roles for metal ions in activating ribozyme catalysis. In addition to withdrawing electron density from the substrate phosphodiester group, metal ions can influence proton transfer steps through metal-coordinated ligands. Metal ions near an active site can also influence reactions through electrostatic stabilization or destabilization of reactant, product, or transition states.

dx.doi.org/10.1021/cr400476k | *Chem. Rev.* 2014, 114, 4318–4342

Metal ions can also influence reactions without interacting directly with catalytic functional groups.[9] A metal cation in proximity to an active site can change the electrostatic environment, stabilize negatively charged transition states, and/or perturb the pK_a values of functional groups. Coordination of metal ions to nucleobases withdraws electron density, thereby affecting the pK_a values of other substituents in the ring. Both the hairpin ribozyme and the ribosome are thought to promote catalysis without utilizing a catalytic metal. However, divalent metals are still important for folding of these RNAs and, therefore, could aid in defining the electrostatics of the active site and provide other long-range effects.[9]

3. METHODS USED IN RIBOZYME STUDIES

3.1. Subdomains and Active Constructs

Ribozymes and other functional noncoding RNA systems are frequently studied as subdomains that represent truncated sequences isolated from their natural context. Much as membrane proteins are sometimes truncated to form soluble domains, these RNAs form discrete folded structures and are designed to maintain the activity of interest. As with truncated proteins, however, it is helpful for the reader to keep the natural context in mind.[24] Some ribozymes, such as RNase P, have been studied as the RNA component of an RNA−protein holoenzyme. In addition, the smaller nucleolytic ribozymes such as the hammerhead and hairpin ribozymes are often studied as truncated constructs that represent the minimal catalytic unit. For mechanistic studies, these, and the hepatitis delta virus and other ribozymes, have also usually been redesigned from natural cis-cleaving systems to RNAs that cleave a substrate in trans conformation. The re-engineering of naturally occurring ribozymes has enabled great insights into the fundamentals of RNA catalysis. In the case of the hammerhead and hairpin ribozymes, early truncated constructs are acknowledged to have lost tertiary interactions that aid in folding, thereby obfuscating the individual contributions of metal ions to folding and catalysis; later constructs reinstated these properties.[24,25]

3.2. Strategies for Detecting RNA−Metal Interactions

Several function-based biochemical approaches have been developed to help identify and isolate the roles of metal ions in RNA catalysis. Because RNA requires cations to fold, it is generally impossible to do a deletion experiment that entirely removes active-site electrostatic contributors. On the other hand, a popular approach has been to compare the effect of cation identity on the rate of ribozyme catalysis. Replacing Mg^{2+} with monovalent ions such as Na^+ or Li^+ changes the charge, size, and coordination behavior of the supporting cation. Monovalent cations, including NH_4^+, can support significant activity in several of the Class II ribozymes, but only under nonphysiological conditions of >1 M added cation. This observation alone does not negate the importance of a cation in the active site, and it also does not logically refute the necessity of Mg^{2+} under physiological conditions. However, for cases such as the hammerhead, hairpin, and GlmS ribozymes for which very high concentrations of monovalent cations can support varying levels of ribozyme activity, it has also been found that conserved nucleobases play intimate roles in the reaction. Taken together, these observations indicate that such ribozymes have multiple types of groups that contribute to the catalytic center, allowing function to be supported by cations with a variety of properties. In the case of the hairpin and GlmS ribozymes, all current evidence indicates that cations do not directly contact active-site groups, although nearby structural metal ions might exert an electrostatic influence. The hammerhead ribozyme maintains an important Mg^{2+} ion (discussed below). Of note, the hairpin and GlmS ribozymes are also fully active in $Co(NH_3)_6^{3+}$, the exchange-inert structural equivalent of fully hydrated Mg^{2+}, whereas the hammerhead and hepatitis delta virus ribozymes are not.[8]

By contrast, the large group I, group II, and RNase P ribozymes are not active in high molar concentrations of monovalent cations and have a distinct requirement for divalent cations. Current models for the group I and group II intron active sites show an intricate set of Mg^{2+} ions that are mainly coordinated by phosphodiester groups and are reminiscent of the carboxylate-coordinated Mg^{2+} ions found in polymerase active sites. Because these larger ribozymes perform multiple reactions, they might have developed "universal" active sites that minimize requirements for rearranging when binding new substrates.

A powerful method for probing possible inner-sphere coordination sites is to create substitutions of functional groups that introduce biochemical and spectroscopic specificity. Sulfur substitutions of phosphate oxygens to create phosphorothiolate (bridging oxygen) and phosphorothioate (nonbridging oxygen) groups decrease the affinity of hard metals such as Mg^{2+}, resulting in decreased activity of the ribozyme if that metal−oxygen interaction is important for ribozyme function.[16,26,27] If the addition of a thiophilic metal such as Cd^{2+} rescues catalysis, there is strong evidence for inner-sphere coordination at that site. Substitution of a 2′-OH to a 2′-NH_2 is another method that can reveal 2′-coordination through enhanced interaction with softer metals. These substitutions, however, are not sterically equivalent to oxygen, and therefore, a different ionic radius can perturb an active site and potentially affect catalysis without showing rescue. Thus, although observation of metal rescue might be a good predictor of a specific metal-ion site, the absence of rescue does not necessarily exclude relevant inner-sphere coordination.

The phosphorothioate substitution also provides a marker for ^{31}P nuclear magnetic resonance (NMR) studies, because the sulfur atom induces a 50−60 ppm downfield shift in the ^{31}P signal from the substituted site. Coordination of the phosphorothioate by diamagnetic Cd^{2+} results in an *upfield* shift, providing direct observation of this interaction (reviewed in ref 17). Other spectroscopic techniques, including proton NMR, electron paramagnetic resonance (EPR), and X-ray absorption spectroscopies can in some cases be used for more direct observation of metal-ion associations with RNA in solution (reviewed in refs 17 and 18).

Identifying metal ions and their ligands by X-ray crystallography is a powerful but difficult business in complex RNAs. As has been noted,[3] data interpretation regarding metal sites is aided by high resolution, which is less available for RNA structures than for proteins given the dynamic nature of the RNA backbone. Mg^{2+}, the RNA "metal of choice", has a low electron density that can make discrimination from disordered water a challenge. Metal-ion substitution, preferably with anomalous scattering, is a gold standard for metal-site identification by X-ray crystallography. Given sufficient resolution to obtain distances and geometries, whether a particular metal is making contact with surrounding ligands through inner-sphere or outer-sphere contacts can be inferred. However, a crystal is a still picture of a dynamic molecule,

dx.doi.org/10.1021/cr400476k | *Chem. Rev.* 2014, 114, 4318−4342

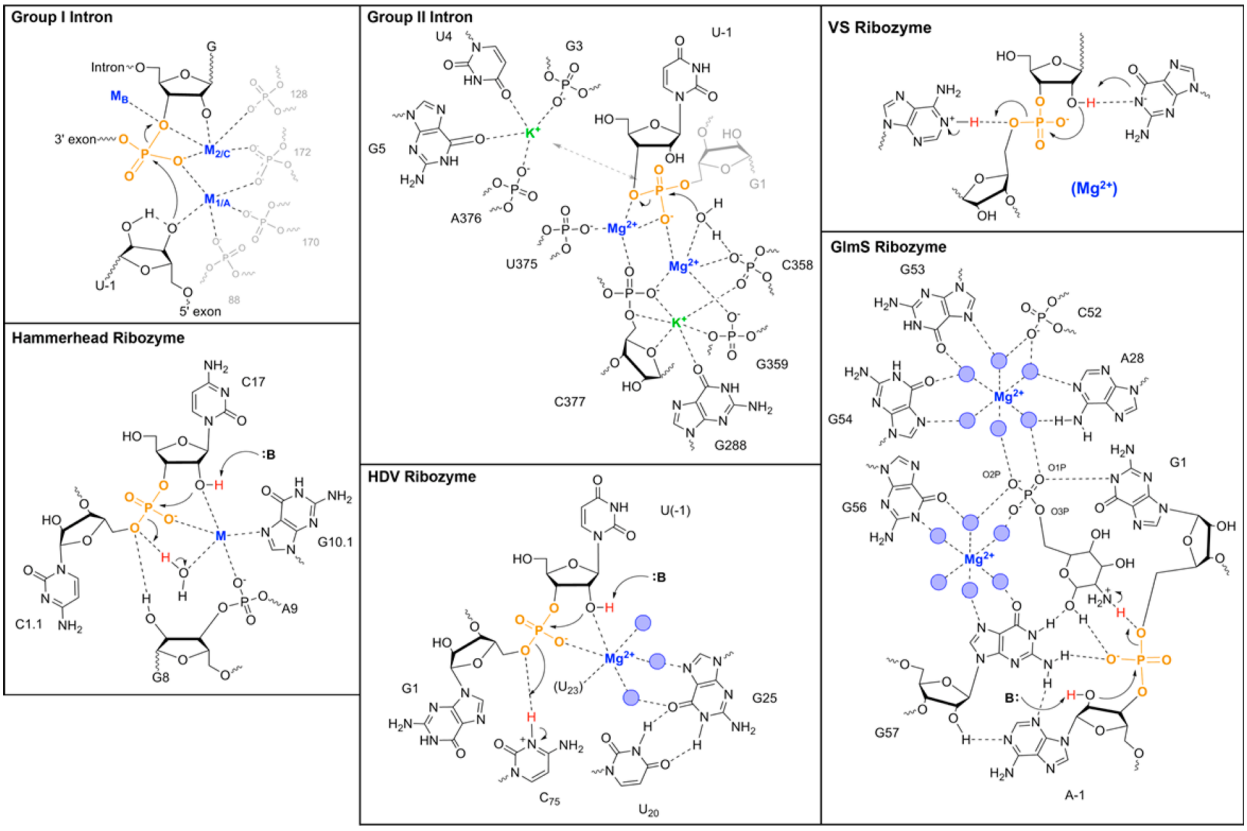

Figure 4. Active sites of ribozymes. Current proposals for the ground-state structure of each ribozyme are based on experiments as reviewed in each section below. Highlighted are (gold) the phosphodiester bond substrate of each reaction, (blue) Mg^{2+} ions at or near the active site, (green) K^+ ions located in the group II intron, and (red) protons either removed or donated in the reaction. The group II structure represents the second step of the splicing.

which also is often altered to facilitate crystallization, and substituted metal ions might have coordination properties that differ from those of Mg^{2+}. Ribozymes must often be designed to incorporate debilitating substitutions to facilitate crystallization and, therefore, might lose interactions needed to properly position the active site. Local RNA structure is often based on networks of interactions and can be quite sensitive to changes in hydrogen bonding and other substitutions. Thus, as is the case with protein enzymes but perhaps even more so with ribozymes, the compelling information gained from X-ray crystallography must be carefully analyzed with respect to corresponding biochemical data.

Computational approaches have the potential to deepen understanding of reaction pathways and the contributions that have been evolved in RNA that direct specific reactions.[28,29] The electrostatic properties of RNA, along with the breadth of available conformational landscape,[30] provide unique challenges to developing these methods for RNA. Great progress has been made in recent years, and the field is developing its own version of the blind CASP (computer-aided structure prediction) challenge for RNA structure prediction. With the availability of higher-resolution X-ray structures as starting points, hybrid quantum mechanics/molecular mechanics (QM/MM) approaches are being applied to ribozymes that incorporate metal-ion cofactors to calculate reaction trajectories.[29,31] In addition to reaction trajectories, such approaches could deepen the understanding of proton networks in these sites[31] and contributions of the RNA environment to electronic properties of RNA functional groups, topics that are particularly challenging to access experimentally. Because of the challenges noted above in X-ray structure analysis and theoretical modeling of RNA properties, there is great emphasis on coupling theoretical approaches closely with experimental predictions and verification.

4. OVERVIEW OF RIBOZYMES REVIEWED

In the subsequent sections, current mechanistic proposals for the majority of naturally occurring ribozymes are presented. Figure 4 provides a composite summary of the ground-state active sites for six of these catalysts.

First described are the "large" group I and group II introns, with active sites consisting largely of Mg^{2+} (and K^+, in the case of group II) ions mounted on a scaffold of phosphodiester backbone ligands. Next in line is RNase P, which occurs in nature with at least one protein cofactor and catalyzes tRNA 3′-end processing with its RNA subdomain. These three ribozymes in general occur as large RNAs of several hundred nucleotides and, in the case of the group I and II introns, catalyze two separate reactions in the act of splicing. Subsequently, two "small" nucleolytic ribozymes whose activity is supported by a combination of metal ions and RNA nucleobase contributions are described; these are the hepatitis delta virus and hammerhead ribozyme. The GlmS ribozyme/riboswitch is included as an example of a cofactor-supported RNA catalyst, and it might have electrostatic but indirect influences from bound metal ions. The hairpin and *Neurospora* VS ribozymes appear to use similar nucleobases in their active sites, but the pH-dependent behaviors of their reactions differ,

dx.doi.org/10.1021/cr400476k | *Chem. Rev.* 2014, 114, 4318−4342

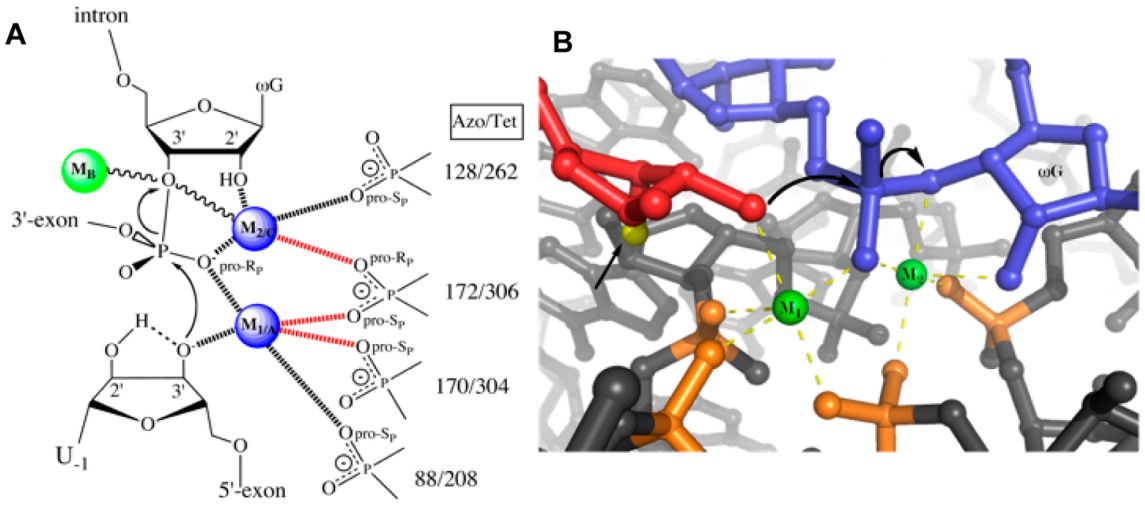

Figure 5. Proposed metal−RNA interactions in the active site of the group I intron during the second step of splicing. (A) Two possible models have been proposed. Based on quantitative analysis of metal rescue experiments, a three-metal model includes $M_{1/A}$ coordinating the 3′-nucleophile and the *pro-*R_p O of the scissile phosphate, M_B coordinating the 3′-leaving group, and $M_{2/C}$ coordinating the *pro-*R_p O and 2′-OH of the cleaved ribose. Alternatively, a two-metal model has been proposed based on crystallographic structures in which $M_{2/C}$ accounts for the observed biochemical interactions of both M_B and $M_{2/C}$. Additional interactions of these catalytic metals with the phosphate backbone of a conserved "M" motif are shown. Nucleotide numbers of the M motif are given for both the *Azoarcus* and *Tetrahymena* sequences. (B) Crystal structure (PDB 1ZZN) of the *Azoarcus* group I intron active site showing the nucleophile (red) attacking the 3′-intron junction (blue) and the interactions of $M_{1/A}$ and $M_{2/C}$ (green) with both catalytic groups and the M motif (orange). A 2′-OMe (yellow with arrow) substitution was used in this crystallization construct.[38]

posing an unresolved mystery for these catalysts. Finally, we include an in vitro evolved ribozyme, the Diels−Alderase, as an example of the breadth of reactions available in RNA catalysis, and conclude with DNA catalysts.

5. GROUP I INTRON

The group I intron from the ciliate *Tetrahymena* pre-rRNA was the first ribozyme to be discovered.[32] Since the initial discovery, group I introns have grown into a class of ribozymes that are defined by a conserved core and several conserved domains and are found in a range of organisms including prokaryotes, eukaryotes, and bacteriophages.[33] Group I introns catalyze the self-excision of intronic sequences through two separate phosphoryl-transfer reactions. In the first step, the 5′-exon−intron junction is cleaved following attack by the 3′-oxygen of an exogenous guanosine cofactor. This reaction adds the guanosine to the intron and leaves a 3′-hydroxy terminus on the 5′-exon. A structural rearrangement then positions the 3′-intron−exon junction for attack by the newly created terminal 3′-oxygen of the 5′-exon.[34,35] Positioning of the splice site is enabled by a conserved guanosine (ΩG) at the 3′-intron−exon junction, which occupies the same binding pocket as the exogenous guanosine of the first step. The phosphoryl transfer in the second step ligates the two exons in essentially the reverse reaction of the first step and is depicted in Figures 4 and 5. Both reaction steps are proposed to be catalyzed by one active site that is dominantly organized by the intron itself and includes the guanosine binding pocket and conserved metal-ion sites.

The group I introns require Mg^{2+} or other divalent cations for function. Over the ca. 25 years of biochemical and structural studies on this intron, several metal-binding sites inside and outside of the active site have been identified (for a review, see ref 36). Combined with recent structural data, current models of the group I active site reveal a series of phosphate−metal inner-sphere interactions that elegantly organize the ribozyme core through several multidentate metals. From biochemical studies, a working model of the group I catalytic site has long included three metal ions that are predicted to influence the nucleophile, substrate, and leaving group.[36,37] Current crystallographic results support two of three active-site metal ions, finding them positioned as expected for a classic "two-metal mechanism" thought to operate in most protein-based phosphoryl-transfer reactions.[12,36] The differences between these predictions might be due to the model systems used in both structure and function analyses, as described below. For clarity, we have combined the two naming schemes that have been used to distinguish individual metals in the group I intron active site, such that the specificier from crystallography (1 or 2) is followed by that used from metal rescue experiments (A, B, or C).

Several crystal structures of group I introns have been reported, and although most are of the group I intron found in the anticodon loop of pre-$tRNA^{Ile}$ in the purple bacterium *Azoarcus*, there are also structures from pre-rRNA in the ciliate *Tetrahymena* and bacteriophage Twort.[36,38−41] Although all of these structures contain a guanosine in the active site, the inclusion of other active-site components varies. The Twort and *Azoarcus* structures include a 5′-exon (product of the first splicing step).[38,39] *Azoarcus* structures additionally include either the 3′-exon−intron junction (substrate of the second step) or the ligated exons and are debilitated by 2′-deoxy substitutions at various positions or lack the scissile phosphate. One *Azoarcus* structure contains few substitutions, remains active, and captures a "relaxed", postligation active site.[41] Overall, the data agree with structure-mapping studies that the group I intron is composed of three helical domains that stack together to form the active site. Initial structure reports differed, however, in the metal-ion content around the active site of the intron. A buried Mg^{2+} that contacts the leaving group on the 5′-exon was located in the *Azoarcus* and Twort structures ($M_{1/A}$ in Figure 5)[38,39] but not in the *Tetrahymena* structure (which lacks the exon substrate).[40] By contrast, a Mg^{2+} ion contacting the attacking guanosine 3′-OH was located in the *Tetrahymena*

dx.doi.org/10.1021/cr400476k | *Chem. Rev.* 2014, 114, 4318−4342

structure ($M_{2/C}$ in Figure 5) but was substituted by a K^+ ion in the initial *Azoarcus* complex. This difference has been attributed to an indirect consequence of the 2′-deoxy ΩG modification used in creating an inactive, crystallizable *Azoarcus* construct. Although the ΩG 2′-OH position is not directly involved in the reaction, it is hydrogen-bonded to a nucleotide that provides metal-ion coordination; loss of this interaction opens up the site, allowing substitution of Mg^{2+} by the larger K^+ ion. When a native 2′-OH guanosine is present, $M_{2/C}$ is populated as a Mg^{2+} ion and is located within coordination distance of both the guanosine 2′-OH and 3′-OH. Interestingly, the "three-metal mechanism" proposes that these two positions are coordinated by two separate metal ions. It is not possible, however, to easily place an additional metal M_B into the current structures without requiring some structural rearrangement. With M_B modeled into the 3.4-Å *Azoarcus* structure, the closest phosphates (wG206 and C +2) are 3.5 Å away, too far for inner-sphere coordination.[41] Furthermore, there is no biochemical evidence to support a role for these phosphates in metal-binding or splicing activity.

Metals $M_{1/A}$ and $M_{2/C}$ are found at the peaks of a curious, but conserved, M-shaped bend in the RNA backbone that organizes a total of five metal cations.[36] Four of these five core metals make direct contacts with phosphates of the P4−P6 domain, which alone does not contain the active site but acts as the scaffold on which the two other domains pack.

In evaluating the relationship between group I intron crystal structures and models from biochemical analyses, it is important to note that each experimental system samples different steps in the reaction pathway. Both splicing reactions can take place using an active site that is largely conserved, but some structural rearrangements to accommodate different substrates are certainly possible. Most biochemical assays use a group I intron ribozyme that models the first step of the reaction. A large "enzyme" RNA is annealed to an exogenous short oligonucleotide that mimics the 5′-exon substrate, and the reaction is activated by the addition of an exogenous guanosine. The prediction of three separate catalytic metal ions is based on a series of metal-specificity experiments, in which one or a subset of potential metal-ion ligands in the ribozyme core are substituted to alter their metal-ion preferences. The X-ray structures, by contrast, are of ribozymes either without exogenous substrates or monitoring steps in the second reaction. The single X-ray structure showing both metals $M_{1/A}$ and $M_{2/C}$ is of a ribozyme poised for the second reaction step but inhibited by 2′-deoxy substitutions at nearby residues or a lack of the scissile phosphate.[38] To reconcile the crystallography, which monitors a ground-state structure, with the biochemical studies, which can also probe effects on the transition state, one must propose (a) introduction of an additional metal ion and rearrangement in a structure closer to the transition state of the reaction, (b) an influence on the metal-ion occupancy of the perturbations used in either technique, or (c) a slightly different metal-ion content and local structure in the first step of the reaction than in the second. The last situation could derive in part from active-site relaxation and the release of M_B along with the 5′-intron product after the first strand scission. The role that M_B would have played in nucleophile activation would no longer be required, as $M_{1/A}$ is now positioned for activation of the second nucleophilic attack. Overall, the current high level of information concerning the group I intron active site highlights the importance of combining results from multiple approaches and constructs in RNA structure−function analysis. It is moreover astonishing that in the context of a >300-nucleotide ribozyme, the majority of functional metal-ion contacts were picked out by biochemical methods and also observed crystallographically as specifically populated metal-ion sites.

6. GROUP II INTRON

The group II introns are the second largest of the naturally occurring ribozymes and are an extremely diverse family with a strong relationship to the eukaryotic splicing machinery. In vivo, group II introns often have protein cofactors, and only a subset depend solely on RNA for efficient catalysis. Like the group I introns, the group II introns are class I ribozymes, catalyzing two consecutive phosphoryl-transfer reactions between nonadjacent nucleotides. Unlike the group I introns, in group II introns, the initial nucleophilic attack on the 5′-exon junction is performed by either an endogenous 2′-OH group (as opposed to attack by the 3′-OH attack of an exogenous nucleotide in group I introns) or a water molecule, leading to a lariat or linear intermediate, respectively. The second reaction, as for the group I intron, uses the 3′-OH leaving group of step one to attack the 3′-exon junction, excising either a circularized or linear intron. Both phosphoryl-transfer reactions are highly reversible, and the intron can be designed to target any sequence.[42,43]

Group II introns have the additional ability to use DNA as a natural substrate for the reverse reaction. Some group II introns contain open reading frames that code for a reverse transcriptase "maturase". Excised group II introns can use the highly reversible nature of their reactivity to invade duplex DNA in a process called "retrohoming".[44] The intron-encoded maturase then uses the intron RNA as a template for reverse transcription, creating the complementary DNA strand and thereby embedding a DNA copy of the ribozyme into the genome. Thus, group II introns can be mobile genetic elements, effectively "genomic predators" that might be the source of a significant amount of genomic diversity.[45]

Group II introns have a generally conserved secondary structure with highly conserved core elements, the most significant being the D5 helix. This helix contains a "catalytic triad" 5′-AGC-3′ motif that, in the context of a highly organized surrounding structure, is considered the relative of the active site of the spliceosome predicted to reside in the U6 spliceosomal RNA. Although the group II introns have a strict requirement for divalent metals for activity, the family is so diverse that optimal cation concentrations for in vitro activity have been found to range between 0.1 and 100 mM Mg^{2+}.[46] Despite this large range of metal dependencies, several metal-binding sites have been discovered in the most conserved domains of the group II introns, including D5 and D6.[46,47] After years of biochemical and phylogenetic studies, the general global structure of the group II intron and several metal-binding interactions within the core of the ribozyme are becoming clearer, and recent crystal structures corroborate proposed mechanistic models of a multinuclear metal-based catalytic mechanism.[45,48−53]

Several metal-rescue experiments have been performed on the *Saccharomyces cerevisiae* aI5 gamma intron to determine the function of metal ligands within the active site. As is the case for the group I introns, metal rescue was demonstrated for the leaving-group oxyanion in both group II intron steps, demonstrating the importance of metal coordination in stabilizing the charge accumulation on the 3′-leaving group.[18]

dx.doi.org/10.1021/cr400476k | *Chem. Rev.* 2014, 114, 4318−4342

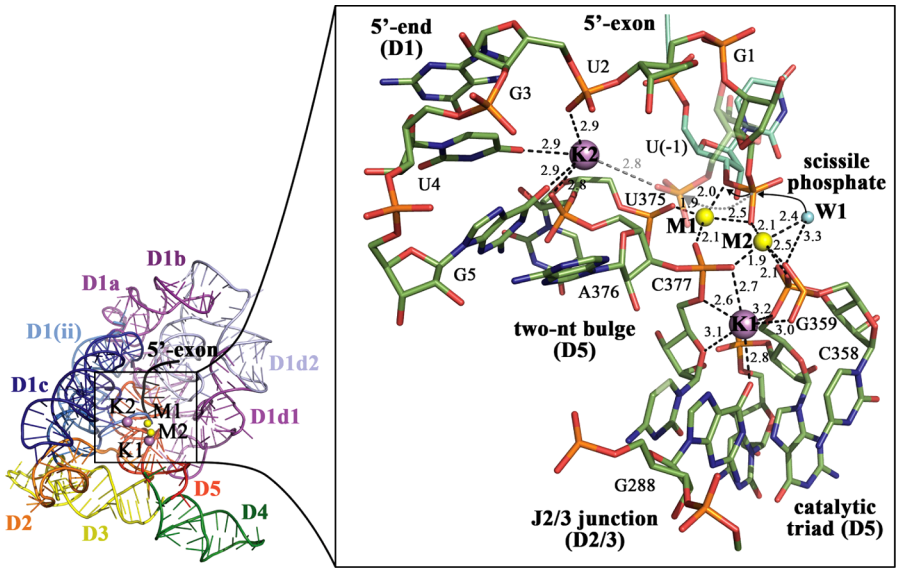

Figure 6. Active site of the *O. iheyensis* group II intron showing activation of the substrate by two Mg^{2+} ions (yellow). Two K^+ ions (purple) are also present, and it is proposed that K2 stabilizes the phosphate product following the cleavage reaction (gray dashed line). Reprinted with permission from ref 45. Copyright 2012 Cell Press.

At the substrate phosphodiester positions, whereas a *pro-*R_p nonbridging oxygen to sulfur substitution showed debilitating defects in both phosphoryl-transfer steps, the pro-S_p substitution had a slight defect only in the first transfer step, signifying that the active sites formed in the two steps are potentially dissimilar.[48,49] Interestingly, the *pro-R* substitution, although inhibiting catalysis, could not be rescued by thiophilic metals, leaving the possibility of specific coordination technically indeterminate.[50]

Interactions of metals with the attacking nucleophile were also investigated for the second step of splicing. These experiments again used sulfur substitution, but they monitored the reverse reaction because sulfur is a poor nucleophile for a phosphorus center.[52] Based on the principle of microscopic reversibility, metal rescue of the leaving group in this reverse reaction indicates that a metal activates the nucleophile in the second step of the forward splicing reaction.[52] Combined with the identified metals stabilizing the leaving-group oxyanion and the possible interactions with nonbridging oxygens of the scissile phosphate, it seems that, like the group I intron, the group II intron uses at least a two-metal mechanism for the second step of splicing.

A 2008 crystal structure of a group II intron from the halotolerant bacterium *Oceanobacillus iheyensis* at 3.1-Å resolution supported the positioning of two metals within the active site in a manner very similar to that observed in the group I intron structures and in agreement with the proposed general two-metal mechanism.[53] The *O. iheyensis* crystal structure, which includes neither of the exons, portrays the intron following the second step of splicing. This reaction step is chemically more similar to the group I reactions, and indeed, the metal ions are positioned solely by bridging and terminal phosphodiester ligands in a manner nearly identical to that observed for group I.

Further crystallographic analysis of *O. iheyensis* in different stages of the reaction confirmed occupancy of these two active-site metals and extended the model to include two K^+ ions in addition to the two Mg^{2+} ions (Figures 4 and 6). This study, through a set of 14 different structures solved with various cations, anomalous scattering, and different substrates, provides a thorough working model for group II intron catalysis.[45] The two Mg^{2+} ions (Ca^{2+} in some structures) contact the reactive groups. The attacking aqua ligand in the first step of splicing is proposed to be coordinated to one Mg^{2+} ion, which also coordinates a nonbridging phophodiester group of the substrate. A second Mg^{2+} ion also coordinates the scissile phosphate along with the leaving group of the first reaction. The two additional well-ordered K^+ ions, one of which shares a bridging phosphodiester oxygen ligand with the nucleophile-coordinating Mg^{2+} ion, would impart additional electrostatic modulation at the active site beyond the roles of the Mg^{2+}. Based on a structure of the cleaved product, it is proposed that one role for K^+ is to stabilize the phosphate product of the first step of splicing.

The unusual $2Mg^{2+}/2K^+$ extended cluster in the group II intron active site is present in the absence of substrate, meaning that, as is appropriate for a genetic predator, the intron is preloaded for function.[45] Interestingly, group II function in vivo has been linked to intracellular Mg^{2+} concentrations.[54] Moreover, it is proposed that lower Mg^{2+} concentrations in subcellular organelles, such as the nucleus, can be a limiting factor to group II activity in higher eukaryotes[55,56] and is linked to the evolution of protein cofactors for this ribozyme.

7. RNASE P

RNase P catalyzes the cleavage of a specific phosphodiester bond during the 5′-maturation of tRNA, cleaving off a "leader" sequence to yield 5′-phosphate-terminated tRNA. In vivo, the holoenzyme contains an RNA subunit and one or more protein subunits.[57] In 1983, RNase P was defined as a ribozyme when it was discovered that the RNA subunit alone was active in vitro.[58] RNase P catalyzes the attack of a phosphodiester bond in the 5′-leader sequence of pre-tRNA by an exogenous water or hydroxide nucleophile. Distinct from the other nucleolytic ribozymes, the products of the RNase P reaction are a tRNA with a 5′-monophosphate and a leader sequence with a 3′-OH terminus. Also, unlike other naturally occurring nucleolytic ribozymes that catalyze reversible but single intrastrand

dx.doi.org/10.1021/cr400476k | *Chem. Rev.* 2014, 114, 4318−4342

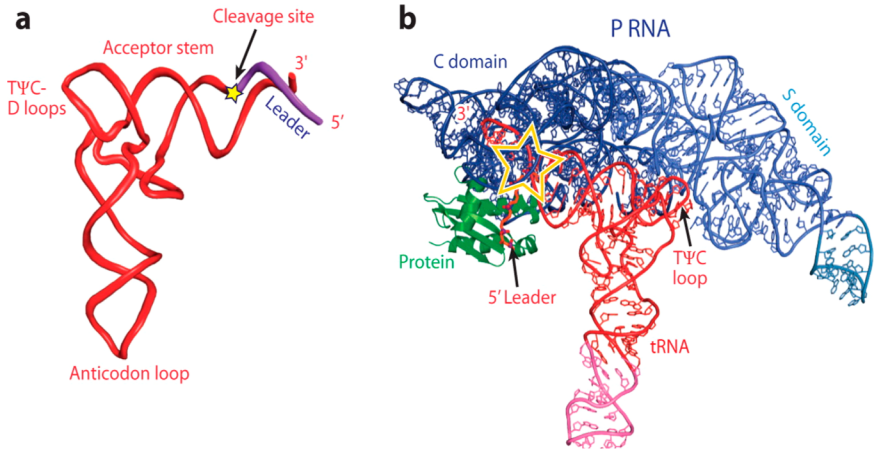

Figure 7. $tRNA^{Phe}$ and RNase P holoenzyme from *T. maritima*. Left: tRNA showing 5′-leader sequence cleaved by RNase P. Right: Structure of product-bound RNase P holoenzyme (PDB 3Q1R) with PRNA (dark blue) and protein (green) and products of tRNA (red/pink) and cleaved 5′-leader sequence (orange). The active site is depicted within a yellow star. Reprinted with permission from ref 57. Copyright 2013 Annual Reviews.

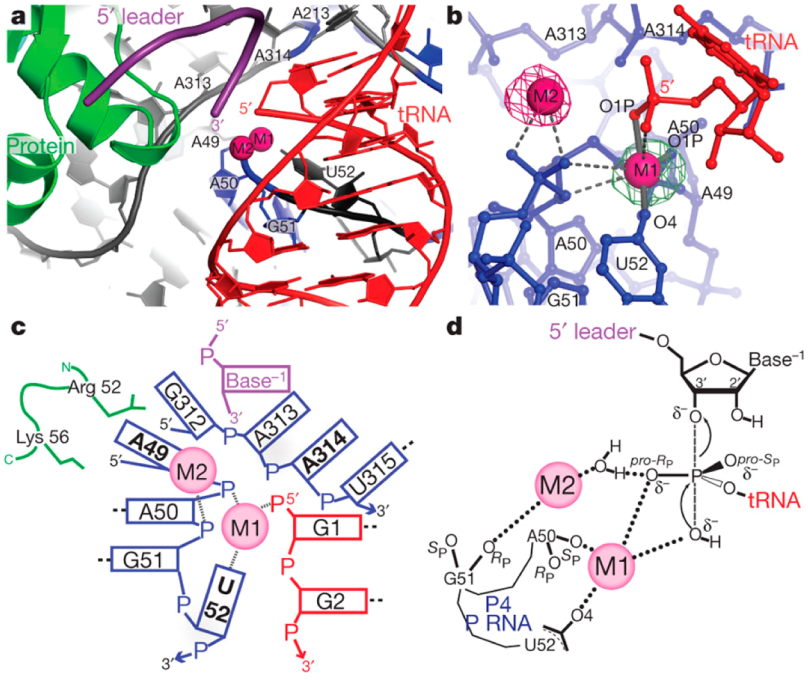

Figure 8. Active site of *T. maritime* RNase P holoenzyme in complex with tRNA and 5′-leader products. (a,b) Structure 3Q1R at 4.1-Å resolution. Ion M1 density (green) appears after soaking tRNA-bound form with Eu(III). (c) M1 is bound to conserved U52 and a phosphodiester ligand and (d) is proposed to bind a nonbridging oxygen of the scissile phosphate and also deliver a nucleophile water/hydroxide for the reaction. M2 appears after addition of the 5′-leader product with Sm^{3+} and is proposed to increase substrate affinity and organize the active site. Reprinted with permission from ref 81. Copyright 2010 Nature Press.

cleavage reactions, RNase P catalyzes multiple turnovers in nature and, therefore, can be considered a true enzyme. In addition to tRNA, RNase P is able to process several other types of naturally occurring RNAs. Protein-only RNase P molecules have only recently been discovered in a handful of systems, including human mitochondria and plants.[59−61] With these few protein-only exceptions, the RNA-protein RNase P complex is ubiquitous in nature, occurring in all three kingdoms of life.

RNase P RNA (PRNA) consists of highly conserved core domains and additional regions that vary depending on the biological source. The diversity of PRNA sequences along with differences in protein cofactors and substrate specificities creates a complex picture of the enzyme in terms of folding, substrate docking, and activity. Simplifying the situation, a majority of biochemical and structural studies have been performed on bacterial RNase P, which has only one protein cofactor. Bacterial RNase P species are classified as ancestral (type A, examples including *E. coli* and *T. maritima*) and *Bacillus* (type B). Recently reported structures of PRNA from *Thermatoga maritima*[62] (Figure 7) and *Bacillus stearothermophilus*[63] show strong similarities in the overall RNA fold from these two different classes, as predicted by previous studies.[57] Until recently (vide infra), only separate structures existed for bacterial P proteins as well as the pre-tRNA substrates. These structures have been used in combination with biochemical, phylogenetic, and computational analyses to provide theoretical models for the RNase P holoenzyme with bound sub-

dx.doi.org/10.1021/cr400476k | *Chem. Rev.* 2014, 114, 4318−4342

strate,[64−66] predicting that the protein cofactor approaches the active site and makes contacts that help position the substrate tRNA. Not surprisingly, then, although PRNA alone can be catalytic, addition of the protein changes properties such as substrate binding and requirements for metal ions. Certain characteristics of the reaction that relate to the mechanism, such as pH dependence and sensitivity to active-site phosphorothioate substitutions, remain generally the same with and without the protein cofactor, indicating that the same basic mechanism is used in reactions catalyzed by RNA-only and holoenzyme RNase P.

RNase P RNA has been shown to be dependent on divalent metals for correct folding, substrate recognition, and catalysis.[67,68] A much-cited result is that approximately 100 Mg^{2+} ions associate with the 300+ nucleotides of PRNA,[67] a number not surprising as a reflection of the mobile counterion atmosphere condensed around an oligonucleotide of this size. As with all ribozymes, picking out the specific contributions of individual ions to catalysis is quite a challenge. The activity and folding of PRNA in several divalent metal combinations suggests that there are both structural and catalytic requirements.[69−71] For instance, Pb^{2+} is unable to properly fold the enzyme,[69] and Sr^{2+} is unable to efficiently promote catalysis despite mediating proper folding.[70] The two in combination, however, demonstrate cleavage.[71] These data suggest that two classes of ions are required for efficient catalysis, one to provide structural stability and the other to activate the nucleophile.[70,71] Addition of the P protein to PRNA increases the affinities of Mg^{2+} ions involved in the reaction.[79] In both PRNA and the holoenzyme, $Co(NH_3)_6^{3+}$ alone cannot support activity, indicating the requirement for inner-sphere metal−RNA interactions.

At this time, there is positive evidence for direct metal-ion contacts with a nonbridging oxygen of the pre-tRNA scissile phosphate and for a metal hydroxide as the attacking nucleophile (Figure 8d). Rescue experiments using sulfur substitutions in the scissile phosphate of precursor tRNA substrates indicate an inner-sphere coordination to the *pro-R* nonbridging oxygen.[72−76] Interestingly, the S_p substitution also interrupts cleavage but cannot be rescued with thiophilic metals. Instead, this substitution results in infidelity of cleavage activity, which targets the 5′-neighboring linkage at a greatly reduced rate.[74,76] Similar behavior is observed when the 3′-oxyanion leaving group is substituted as a substrate phosphorothiolate.[77] The latter behavior contrasts with results of leaving-group rescue experiments in the group I and II introns, which show ready thiophilic rescue behavior of the substituted leaving group.

The RNase P reaction rate increases linearly with pH between 5 and ∼8, an observation that alone signals only a deprotonation step but is also suggestive of the formation of hydroxide or metal hydroxide as the nucleophile. In a rare application of heavy-atom isotope effects to ribozyme catalysis, Harris and co-workers measured the characteristics of $^{18}O/^{16}O$ incorporation into the RNase P product and compared them to values for hydroxide- and Mg^{2+} hydroxide-catalyzed phosphodiester hydrolysis, as well as the Zn^{2+}-catalyzed ADA reaction.[80] Their results showed a remarkably similar, positive solvent isotope effect for the RNase P and Mg^{2+}-catalyzed model reactions. This value, slightly lower than that observed for the model reaction in the absence of Mg^{2+}, suggests a vibrational "stiffening" of the OH^- nucleophile that is consistent with coordination to the Mg^{2+} ion in RNase P. As the authors noted, their study could not formally exclude the possibility of a hydrogen-bonded OH^- in the ribozyme active site, but the strong coincidence between values for the Mg^{2+}-based model system and the ribozyme argues in favor of a parallel reaction mechanism.

The apparent coordination of Mg^{2+} to the tRNA phosphodiester bond in the RNase P reaction site might be predicted to catalyze the same internal cleavage reaction as in other nucleolytic ribozymes. Thus, an interesting question for RNase P is how the substrate 2′-OH group is discouraged from acting as its own internal nucleophile, a reaction that would result in an incorrect 5′-OH tRNA product. To achieve the correct 5′-phosphate tRNA product, RNase P thus must both precisely deliver an external nucleophile and also sequester the neighboring tRNA 2′-OH away from competition. Somewhat surprisingly, however, this potentially competitive 2′-OH group at the cleavage site has been shown to be important for catalysis. A 2′-deoxy or 2′-amine substitution affects substrate binding, cleavage rate, cleavage specificity, and metal binding.[78] Whether a metal ion directly coordinates the 2′-OH is unknown. It is possible that the 2′-OH acts in proton donation, eaither as a source or in relay, to the leaving group of the reaction, but this possibility remains to be tested.

A recent set of X-ray structures of bacterial *T. maritima* bacterial RNase P holoenzyme in complex with product tRNA and 5′-leader sequences has added support for metal-ion positioning at the active site of the enzyme.[81] With only the product tRNA bound, a Eu^{3+} ion soaked into the crystal appears bound to ligands on the P4 helix and also the tRNA 5′-phosphate. In a structure containing the additional product, the cleaved leader sequence, and added Sm^{3+}, the Sm^{3+} ion localizes at the 3′-end of the leader sequence and approximately 4 Å from the Eu^{3+} ion (Figure 8). Although these structures have insufficient resolution, at 3.8 and 4.1 Å, respectively, to uniquely identify metal-ion ligands, the general position of the metals is consistent with expectations based on biochemical studies.[57,81] An earlier structure of the bacterial *B. stearothermophilus* RNase P RNA, at 3.8-Å resolution, also located metal ions Os(III) and Pb^{2+} in the general region of P4.[82] To date, no X-ray crystal structure with "native" Mg^{2+} ions is available for RNase P. The available biochemical and structural evidence suggests, however, an active site in which at least one metal ion binds to the scissile phosphodiester bond and also delivers the hydroxide nucleophile for pre-tRNA cleavage. Despite great progress in understanding RNase P, much work remains to be done on this highly conserved system.

8. HEPATITIS DELTA VIRUS (HDV) RIBOZYME

The hepatitis delta virus (HDV) ribozyme (Figure 9) is a class II ribozyme, and like the hairpin ribozyme, it is present in circular subviral RNAs for processing genomic units during rolling circle replication.[83,8] It was originally thought to exist only in the hepatitis D virus, a rare satellite virus of hepatitis B, but numerous HDV-like ribozymes have recently been discovered. For example, the HDV-like CPEB3 ribozyme, first discovered through an in vitro selection method in the human genome, has been shown to be highly conserved in mammals.[84,85] Further, structure-based bioinformatics searches have revealed additional nonmammalian HDV-like ribozymes, and the biological functions of HDV-like ribozymes are being studied in the human genome, the African mosquito, and fruit flies.[85]

dx.doi.org/10.1021/cr400476k | *Chem. Rev.* 2014, 114, 4318−4342

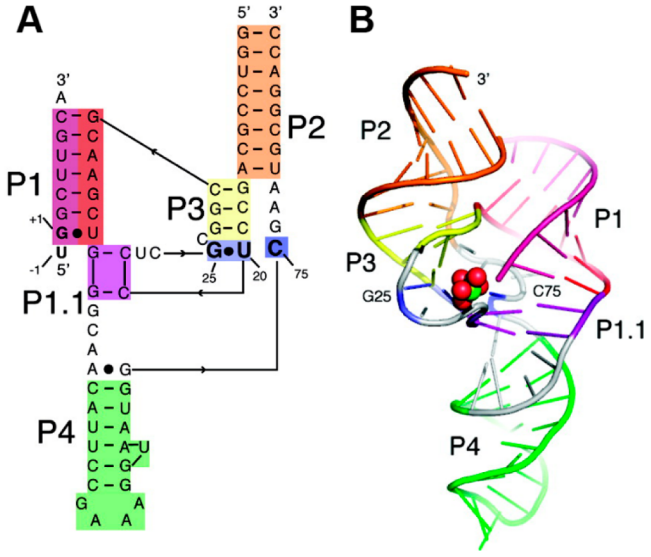

Figure 9. Hepatitis delta virus. (A) Secondary structure of the trans-acting HDV ribozyme used for crystallography. The HDV ribozyme exhibits five paired regions (P1–P4) organized in a pseudoknot structure. (B) Line representation of the crystal structure demonstrating a partially hydrated magnesium ion coordinated to the active site. Reprinted with permission from ref 95. Copyright 2010 American Chemical Society.

Numerous HDV ribozyme crystal structures have been solved. The first structure was solved in 1998 and depicted the ribozyme in a postcleavage state.[86] The ribozyme comprises five paired domains and two pseudoknots that fold into a compact structure, burying the active site. Occlusion of the active site allows rigidity and structural organization, and the HDV ribozyme has comparatively higher catalytic rates than other class II ribozymes.[87]

The early HDV structure supported later biochemical results regarding the catalytic mechanism. In this structure, the N3 of cytosine 75 is positioned to act as a general acid for activation of the leaving group. This hypothesis is supported by the discovery that the pK_a of C75 is shifted near neutral[88] and a C75U mutation is deleterious to ribozyme catalysis.[89] As compared to cytosine, uracil is unlikely to act as a proton donor/acceptor. Imidazole rescues a C75U mutation, demonstrating the importance of protonation to HDV catalysis.[90] Furthermore, a 5′-phosphorothiolate substitution, which creates a hyperactive leaving group, suppressed deleterious C75 mutations, supporting the role of C75 as a general acid.[91]

A metal ion is not observed in the active site of the 1998 structure, which is surprising because the HDV ribozyme utilizes a nonspecific divalent metal ion for catalysis.[8,92] The activity-related metal ion is competitively inhibited by exchange-inert cobalt hexammine, a hydrated magnesium ion mimic, indicating a requirement for inner-sphere coordination.[93] The ribozyme is also active in molar concentrations of NaCl, but with a 3000-fold reduction in activity.[94]

Early precleavage crystal structures have been obtained, facilitated by a C75U substitution, 2′-deoxy substrate strands, or the absence of divalent metals.[89] In these structures, a variety of divalent metal ions as well as cobalt hexammine were shown to be capable of inhabiting the active site of the HDV ribozyme. However, C75U mutants might not represent properly folded ribozyme active sites, as the keto group on uracil does not hydrogen bond with other active site members in the same way as cytosine's exocyclic amine. Also, because uracil cannot be protonated, the electrostatics of the active site are altered from that of a wild-type ribozyme.[8]

The latest crystal structure of the precleavage HDV ribozyme solves the issue of active-site perturbation through the C75U mutation by inhibiting substrate cleavage through deoxynucleotide mutations on the substrate strand.[95] The resulting structure shows a partially hydrated magnesium ion located in the active site, near both the scissile phosphate and C75, interacting through outer-sphere coordination with two water molecules with a G25:U20 reverse wobble. The G:U reverse wobble orientation presents a local negative electrostatic potential orientated on a highly accessible minor groove face, an attractive target for divalent metal ions.[8,96] The Mg^{2+} ion also shows a single inner-sphere coordination to the *pro-Sp* oxygen on U23, and the authors modeled three additional water molecules around the Mg^{2+} ion to complete its coordination shell, but noted that one of these modeled water molecules is likely due to another unresolved inner-sphere coordination, possibly to the substrate strand.[95] Electron density around the scissile phosphate of the inhibitor substrate strand was poor in this construct. The authors were able to conclusively resolve G(1), but a clear picture of the scissile phosphate and U(−1) was not possible due to disorder. Given that cleavage of both the HDV and HHRz ribozymes require local geometries favorable for in-line attack, the authors further developed their HDV precleavage structure by modeling in the cleavage site of the HHRz, guided by the G1 position, and found that the resulting structure is consistent with the crystallographic data (Figure 10).[95]

Based on this model (Figure 10), it is hypothesized that the catalytic magnesium ion interacts through inner-sphere coordination with the 2′-OH group of U(−1), lowering its

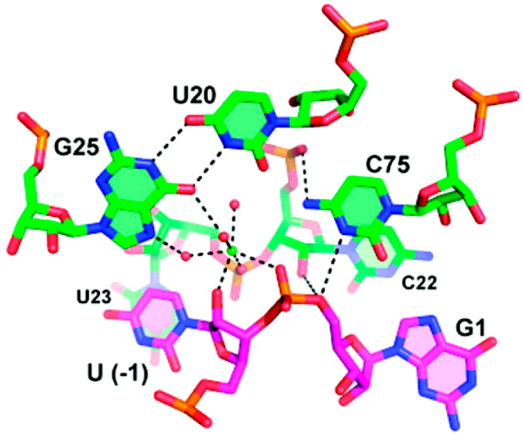

Figure 10. HDV ribozyme active site with a modeled hammerhead scissile phosphate substrate. The HDV structure at 1.9 Å[95] includes electron density for the ribozyme (green), Mg^{2+} ion (green), and nucleotide G1 and others upstream from the cleavage site, but U(−1) and below were disordered. In pink are the nucleotides immediately surrounding the scissile phosphate from a structure of the hammerhead ribozyme, built into the HDV structure using G1 for alignment. This overlay fits the observed HDV electron density and generates a hypothesized model for structure and catalysis that involves coordination of the catalytic metal ion to the 2′-hydroxyl of U(−1) and the *pro-*R_p oxygen of the scissile phosphate. C75 is shown within hydrogen-bonding distance of the leaving group, consistent with a role as the general acid in this reaction. Reprinted with permission from ref 95. Copyright 2010 American Chemical Society.

dx.doi.org/10.1021/cr400476k | *Chem. Rev.* 2014, 114, 4318–4342

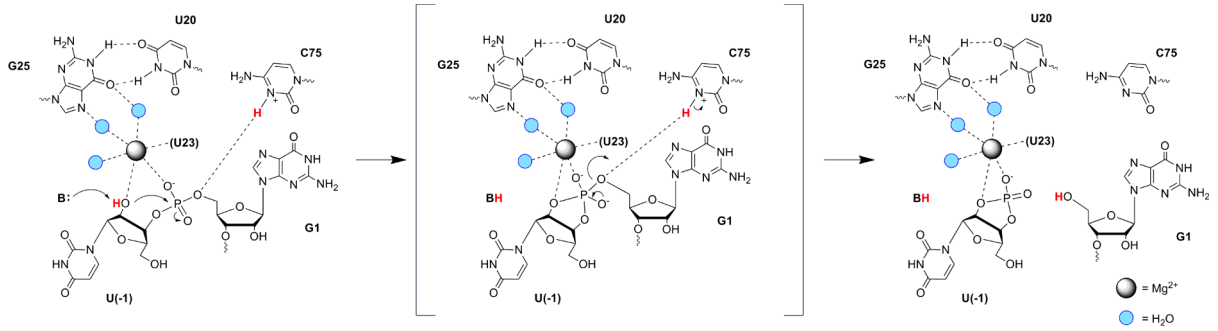

Figure 11. Proposed mechanism for HDV ribozyme catalysis. Under this hypothesis, Mg^{2+} serves to stabilize the building negative charge on the 2′-hydroxyl group of U(−1), activating it for deprotonation by an as-yet-undefined base and nucleophilic attack on the scissile phosphate. The Mg^{2+} is bound through outer-sphere interactions to an electronegative face of the G25:U20 wobble. In the presence of divalent metal ions, the reaction is proposed to be concerted and to pass through a phosphorane-like transition state (ref 98).

pK_a and activating it for nucleophilic attack on the scissile phosphate.[95] This metal ion is also hypothesized to interact with the *pro-*R_p oxygen at the scissile phosphate, in agreement with previous phosphorothioate substitution studies.[97] It is believed that, in the presence of divalent metal ions, the reaction undergoes a concerted mechanism with a phosphorane-like transition state, as supported by quantum mechanical/molecular modeling studies.[98] A full HDV reaction sequence is depicted in Figure 11.

The structure in Figure 10 and the model in Figure 11 preserve the previously described role of C75 as a general acid[8,93] but do not clarify the identity of the general base involved in deprotonation of U(−1). Several hypotheses exist: First, water or hydroxide from the solvent could play a role as a general base and deprotonate U(−1). Alternatively, the 2′-hydroxyl of G27 is in position to hydrogen bond with the 2′-hydroxyl of U(−1) and could be the proton acceptor. The third possibility is that one of the water molecules coordinated to the catalytic Mg^{2+} ion could act as a Brønsted base.[99]

Mutating the G:U reverse wobble to an isosteric A:C reverse wobble results in a significantly less electronegative face. This mutant exhibits a k_{max} decreased 100-fold as compared to that of the wild-type, and an altered pH-rate profile that resembles the wild-type ribozyme in the absence of Mg^{2+}.[99] The authors therefore attribute the mutant's properties as due to loss of the active site Mg^{2+} ion. These data support the model in Figure 11, but the authors note that they do not rule out the possibility that the active site Mg^{2+} could also coordinate a water molecule to act as a Brønsted base, thereby acting as an acceptor of the proton from the 2′-OH group of U(−1).[99]

9. HAMMERHEAD RIBOZYME (HHRZ)

The hammerhead ribozyme (HHRz) is a class II ribozyme that was originally found in viroids, autonomous subviral plant pathogens.[100] As with the other viral-associated ribozymes, the hammerhead ribozyme is required for the processing of unit-length viral genomes during rolling circle replication. The HHRz has since been discovered in the genomes of several higher organisms, [101] including blood flukes and salamanders, as an active discontinuous gene regulator in mice,[102] and in several mammalian genomes including human.[101] Although the biological relevance of HHRz activity in most of these organisms remains unknown, its high conservation suggests as-yet undiscovered functions as a noncoding RNA regulator.[102]

The HHRz is composed of three helices that form a three-way junction with a conserved catalytic core (Figure 12).[103] The majority of early biochemical and structural studies used a minimal HHRz construct containing truncated helices designed to simplify in vitro studies. It was later found that an important tertiary interaction between loops on the helices is phylogenetically conserved, albeit with little primary sequence conservation between organisms.[104] This interaction stabilizes a more compact form of the HHRz and supports higher in vitro rates while lowering the Mg^{2+} dependence of folding to increase in vivo rates as well.[103,105] With some notable exceptions, the results of extensive mutagenesis studies that were performed on the truncated HHRz map to results on the more extended versions of the ribozyme, indicating that the lower rates achieved in the absence of the tertiary interaction reflect a lower population for the active ribozyme but the same overall mechanism.[103]

The activity of the HHRz is strongly dependent on divalent metals when monovalent cations are near physiological concentrations of <150 mM. Confusingly, in molar concentrations of monovalent cations, the *truncated* HHRz can be driven to near-maximal rates.[106] This was an important discovery that helped uncover additional contributors to catalysis in the HHRz. For the extended version of the ribozyme, however, monovalent cations and $[Co(NH_3)_6]^{3+}$ support rates that are orders of magnitude lower than those achievable with divalent cations.[105,107] As described below, metal-rescue experiments provide evidence for functional metals in HHRz catalysis, and crystallography locates metal ions in the active site. Moreover, HHRz reaction rates depend strongly on the identity of the divalent cation.[107,108] Thus, although some activity can be attained in the absence of Mg^{2+}, all indications are that, under physiological conditions, metal ions are a critical component of the HHRz mechanism.

Phosphorothioate metal-rescue experiments on the truncated HHRz identified the *pro-*R_p oxygen of both the scissile phosphate and the A9 phosphate as potential metal sites involved in HHRz catalysis (reviewed in ref 103). In the truncated HHRz construct, analysis of metal rescue of a doubly substituted HHRz linked the A9 and scissile phosphates to a single rescuing divalent cation.[109] In the extended HHRz construct, both of these sites are still sensitive to phosphorothioate substitution,[105] and thermodynamic analysis of Cd^{2+} rescue of the scissile phosphorothioate supports a ground-state metal interaction.[110]

dx.doi.org/10.1021/cr400476k | *Chem. Rev.* 2014, 114, 4318−4342

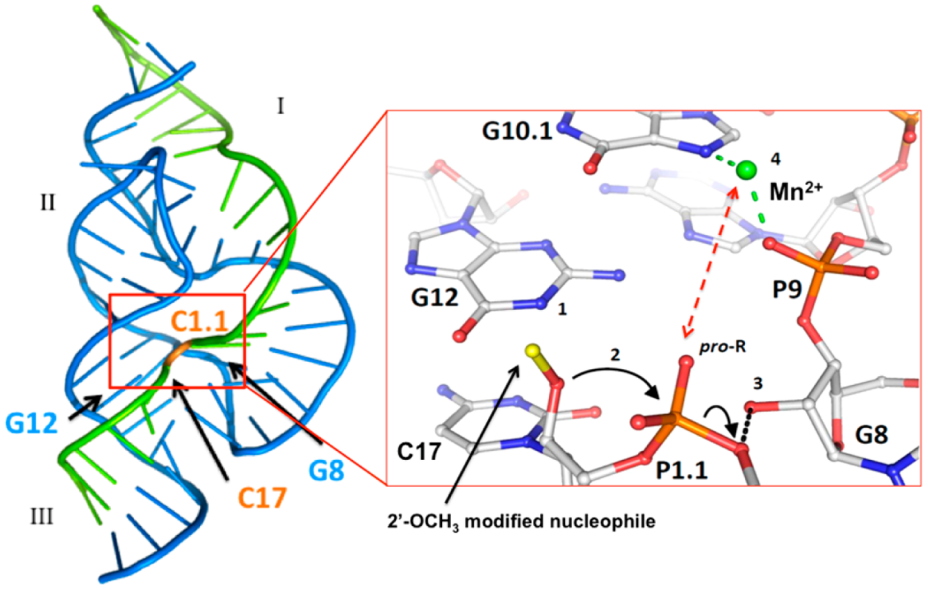

Figure 12. Structure and active site of the hammerhead ribozyme. Structure 2OEU[112] of the *S. mansoni* HHRz sequence showing the active site at the 3-helix junction. At right, structure showing the 2′-nucleophile (substituted as 2′-OMe), scissile phosphate P1.1, Mn^{2+} ion (green), and conserved G12 and G8 nucleobases near the nucleophile and leaving group, respectively. Biochemical studies predict that the metal ion contacts P1.1 in the ground state,[110] and both P1.1 and P9 are predicted to functionally bind metal ions,[105,109] suggesting a slight rearrangement from the crystallographic structure.

Crystal structures of extended HHRz constructs help to reconcile the biochemical data regarding metal interactions within the active site, as well as other functional groups within the RNA. In the newest X-ray structures, the functionally important, and biochemically linked *pro-R* oxygens of A9 and the scissile phosphate are only 4.3 Å apart, a near-ideal distance for a single bridging Mg^{2+} ion.[111,112] However, a Mn^{2+}-soaked structure shows the metal ion coordinated to only the A9 phosphate and the N7 of G10.1.[112] It is possible that the 2′-methoxy group at the nucleophile, used to facilitate crystallization, influences the local structure of the active site.

As reviewed in ref 103, phylogenetic analysis, biochemical studies, and photo-cross-linking experiments all point to the particular importance of two invariant purine nucleobases in the HHRz active site, G12 and G8. Crystallographically, these nucleobases flank the scissile phosphate, with G12 poised within hydrogen-bonding distance of the 2′-nucleophile, and the G8 nucleotide, positioned by conserved base pairing with C3, donating a ribose 2′-OH hydrogen bond to the leaving group.[111,112] These two invariant groups have been proposed to be the general base/general acid actors in the HHRz reaction, with a deprotonated G12 acting as a general base for the 2′-OH nucleophile.[111] However, although the pK_a of G12 has been inferred from chemical cross-linking studies,[113] its high value is difficult to match with the kinetic pK_a values that are needed to model general base deprotonation. Also a mystery is the influence of metal-ion substitutions such as Cd^{2+} on the kinetic pK_a values of the HHRz reaction.[113,114] The bridging metal could potentially interact with the 2′-OH nucleophile[115] and/or the 5′-leaving group as well, as is depicted in the HHRz model shown in Figure 4 of this review. Theoretical studies support a model in which the bridging Mg^{2+} ion makes a significant contribution to the stabilization of the leaving group and activation of the acidic G8 2′-OH group.[116] Like the HDV ribozyme, the HHRz ribozyme appears to use both metal ions and nucleobases in catalysis, but the details of catalysis and synergy between these players are still under investigation.

10. HAIRPIN (HP) RIBOZYME

The hairpin ribozyme motif is a self-cleaving RNA motif embedded in the satellite tobacco ringspot virus.[117,118] Its biological role is to perform site-specific phosphodiester bond-cleavage reactions in the course of virus replication. Like the hammerhead ribozyme, the HP ribozyme was truncated and formulated into trans-cleaving constructs and has served as a model system for investigating RNA catalysis for many years.[117,118] Unlike the hammerhead ribozyme, however, the HP ribozyme does not have a specific requirement for divalent cations. Although cations are required for folding, the HP catalytic center appears to have evolved to use only nucleobases for catalytic support. Thus, the HP ribozyme has served as a model for investigating nucleobase-only catalysis. A great deal of work has been done toward determining the ionization state and microscopic pK_a values of nucleobases embedded in this RNA and comparing them to kinetic properties in a quest to identify their roles in facilitating chemical reactivity, including proton transfer during the HP ribozyme reaction.

The active site of the HP ribozyme contains highly conserved A38 and G8 nucleobases that flank the scissile phosphate (Figure 13). pH−rate profiles of the HP reaction, which are shown in the next section in comparison with those of Varkud Satellite ribozyme (Figure 16), indicate a role for an ionizable group with a pK_a near 6.2 and a second group with a pK_a above 9. The analysis of such profiles can be ambiguous in the absence of alternative identification of one of the ionizable groups. Based on the influence of site-specific modifications, the N1 of A38 was implicated as critical to catalysis,[119] and a reasonable model of a protonated A38 acting as general acid was developed. Similar substitutions around G8 determined the importance of the exocyclic and N1 amine groups, implicating them as hydrogen-bonding contributors in the active site.

The challenge of directly measuring the A38 pK_a value and matching it to the kinetic pK_a was recently approached by two different methods.[120,121] In one approach, the fluorescent base

dx.doi.org/10.1021/cr400476k | *Chem. Rev.* 2014, 114, 4318−4342

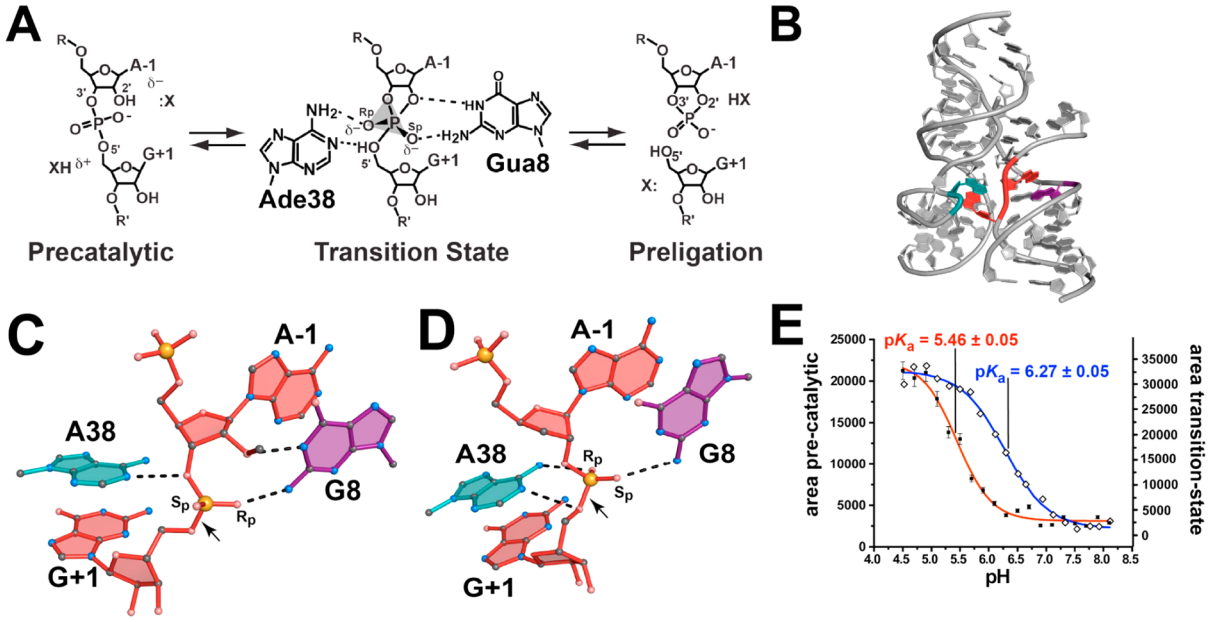

Figure 13. Hairpin ribozyme active site. (A) Reaction catalyzed by the HP ribozyme and proposed contributions of A38 as a general acid and G8 in hydrogen-bond interactions. (B) X-ray crystal structure (PDB 2OUE) with active site A38 in green and G8 in red. (C) Close-up of the 2OUE active site. The 2′-nucleophile is blocked as a 2′-OMe, but accepts a hydrogen bond from G8. The G8 N6 forms a hydrogen bond with the scissile phosphate. In this inhibited precleavage structure, A38 is within hydrogen-bond distance of the 3′-O but not the leaving group of the reaction. (D) Close-up of a transition-state analogue 2P7F. The 2′−5′-linked variant mimics the bond formed between the 2′-nucleophile and the scissile phosphate. In this structure, A38 N1 is repositioned to act as proton donor to the leaving group. (E) Raman crystallography measurement of A38 N1 pK_a in the inhibited (panel C) and transition-state-analogue (panel D) HP variants. An elevated pK_a of 6.2 in the transition-state analogue (blue) matches the kinetic pK_a, suggesting that the kinetic pK_a reflects the transition state of the reaction. Reprinted with permission from ref 121. Copyright 2012 American Chemical Society.

analogue 8-aza-adenine, which maintains activity in the HP ribozyme, was used as an A38 substitution.[120] Protonation decreases fluorescence, providing a direct monitor of the nucleobase protonation state in the context of the HP ribozyme active site. Using this substitution, the pK_a of 8-aza-adenine at position 38 in the HP ribozyme was measured and found to be elevated by 2 units over that of 8-aza-adenine outside the ribozyme active site. An elevated pK_a is consistent with general expectations concerning the influence of a negative electrostatic potential on pK_a values. Moreover, the pK_a value observed for the 8-aza-adenine substitution within the ribozyme active site matches that observed kinetically, linking protonation of the A38 position to the HP reaction.[120]

In a second approach, direct measurement of the A38 protonation state using Raman spectroscopy of HP crystalline samples (Raman crystallography) was used in two different constructs (Figure 13).[121] Interestingly, in a precleavage construct containing an inhibitory 2′-OMe group at the nucleophile, the measured pK_a for A38, although still elevated by over 1 unit from that in solution, was slightly reduced from the rate-dependent value of 6.2. Because the pK_a value determined by monitoring reaction rates could reflect an influence on the transition state of the reaction, the Raman crystallography experiment was repeated on a crystallographically characterized construct that mimics the transition state by including a 2′−5′ rather than 3′−5′ phosphodiester bond. For this construct, the pK_a value of A38 was elevated to 6.2, the same as the value reflected in pH−rate profiles. In further studies, it was found that substituents at the neighboring conserved G8 residue influenced pK_a values at A38. The results of both of these studies underscore the extreme sensitivity of RNA functional groups to the environments established in ribozyme active sites. In the latter study, pK_a shifts of >1 were found in A38 as a consequence of small perturbations at other positions in the HP ribozyme active site. For a pH-dependent reaction, such a functional-group pK_a change could result in an order-of-magnitude difference in reaction rate. Adding a metal ion into such a site, and changing the Lewis acidic properties of the metal ion, could result in large changes in reaction rate through electronic tuning of the RNA substituents.

11. VARKUD SATELLITE (VS) RIBOZYME

The Varkud satellite (VS) ribozyme is a large, naturally occurring nucleolytic ribozyme encoded by the Varkud satellite plasmid, found only in the mitochondria of certain *Neurospora* isolates.[122,123] It is found in conjunction with the Varkud plasmid, a closed-circular DNA plasmid encoding a reverse transcriptase important for the life cycle of the ribozyme. VS ribozyme RNA is transcribed from a VS plasmid DNA template by *Neurospora* mitochondrial RNA polymerase, and as it is transcribed, the ribozyme initiates self-cleavage to form monomeric transcripts. These transcripts are reverse-transcribed by the reverse transcriptase encoded by the Varkud plasmid, forming VS ribozyme (−) strand cDNA.[123]

No crystal structure exists for the VS ribozyme, so current knowledge about the structure has been inferred from chemical probing and mutagenesis experiments.[124] The VS ribozyme is composed of six helical regions organized into a stem-loop on the 5′-end that contains the cleavage site at an internal loop (helix I) and two three-way junctions organized in an H-shape (Figure 14).[125] Mutations disrupting this secondary structure are deleterious to catalysis, but substitution of one base pair for another has little or no effect, suggesting that the secondary

dx.doi.org/10.1021/cr400476k | *Chem. Rev.* 2014, 114, 4318−4342

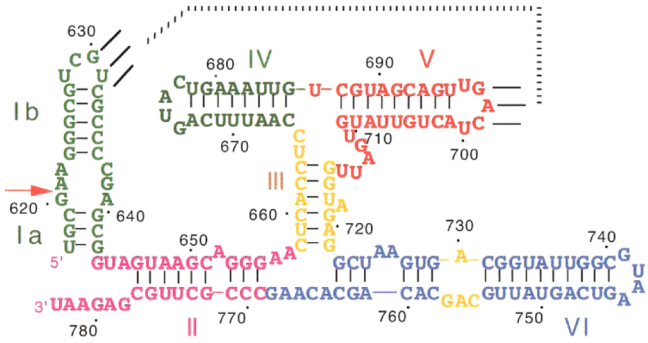

Figure 14. Varkud satellite (VS) ribozyme. Two three-way junctions (among helices II, III, and VI and helices III, IV, and V) give the VS ribozyme an H-shaped structure. The 5′-end is arranged in a stem-loop structure (helix I) and contains the cleavage site in an internal loop (red arrow). Reprinted with permission from ref 124. Copyright 2004 CSHL Press.

structure is more important for activity than the exact sequence.[124]

A model of the VS ribozyme's tertiary structure has been developed using a combination of electrophoretic mobility comparison studies and Förster resonance energy transfer (FRET) spectroscopy on a trans-acting construct (Figure 15).[126,127] Each helical junction appears to undergo Mg^{2+}-dependent coaxial stacking of its two arms, and it is believed that helix I, where the cleavage event occurs, folds into a cleft between helices II and VI. This arrangement fits research showing that the loop of helix Ib contacts the loop of helix V[128] and positions the 5′-end of helix II close enough to the 3′-end of helix I to maintain the connection seen in a cis-acting ribozyme (Figure 15).[124] Perhaps most importantly, this arrangement brings the scission site in close proximity to the A730 loop, believed to be an important part of the catalytic core of the ribozyme.[124,129]

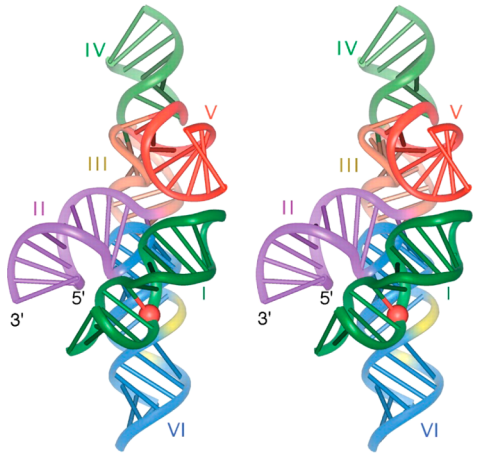

Figure 15. Tertiary structure model of the VS ribozyme based on biophysical measurements. Reprinted with permission from ref 124. Copyright 2004 CSHL Press.

The VS ribozyme active site is believed to be formed by an interaction with the internal loop on stem I (where cleavage occurs) and the A730 loop. Most mutations to the A730 loop result in significant loss of cleavage activity in the trans configuration without causing any major misfolds.[124] Additionally, ethylation protection and phosphorothioate substitutions identified phosphates in the A730 loop that are protected from modification and predicted to be involved in metal-ion binding.[130] A recent NMR structure of a construct containing the A730 internal loop shows an S-turn motif containing two phosphate backbone clusters, which are structures that could bind Mg^{2+} ions.[129] These phosphates are the same as were identified in the prior phosphorothioate substitution studies.[130]

Chemical probing, substitution experiments, and pH–rate profiles have provided an understanding of the players involved in VS catalysis.[131] A756, in the A730 loop, has been shown to be the most sensitive to mutation (Figure 14). Changing it to any other base is significantly deleterious to catalysis in a trans-acting VS ribozyme with little effect on global folding.[127] UV cross-linking demonstrates a strong cross-link between a 4-thiouridine at the scissile phosphate and A756, suggesting that the latter is close to the scissile phosphate in the folded ribozyme.[132] Additionally, G638, across from the scissile phosphate in the internal loop of helix I, is known to be important for catalysis (Figure 14). As with A756, replacement of G638 by any other nucleotide severely impairs cleavage without affecting folding.[133] These results are particularly interesting because the hairpin ribozyme also relies on an adenine and a guanine being brought together through the interaction of distant internal loops, suggesting that they might share similar mechanisms.[131]

In a general catalytic mechanism of a nucleolytic ribozyme, the 2′-hydroxyl group must be activated through deprotonation by a general base, and the 5′-oxygen must be protonated by a general acid. In the VS ribozyme, it is hypothesized that G638 could play the role of the general base and A756 could play the role of the general acid.[131] 5′-Phosphorothiolate substitutions in the scissile phosphate of the VS ribozyme result in a very good leaving group that does not need to be protonated to complete cleavage. This mutation rescues an A756G substitution that normally results in a 1000-fold reduction in cleavage activity, supporting the role of A756 as the general acid. The phosphorothiolate mutations are not significantly affected by modifications to G638, consistent with its role as a general base.[134] Finally, pH–rate profiles, although not conclusive by themselves, suggest a general base with a pK_a of 8.4 and a general acid with a pK_a around 5.2 in the trans-acting ribozyme (Figure 16),[133] whereas pK_a values of 8.3 and 5.8 were observed in a cis-acting ribozyme.[135] A pK_a of 8.6 is consistent with a guanine if its pK_a were reduced by a nearby metal ion, and a pK_a of 5.2 is consistent with an adenine in a particularly electronegative environment.[131] One stipulation with analyzing pH–rate profiles to deduce acid–base catalysis is that the profile observed might be due to a change in the rate-limiting step instead of the ribozyme protonation state. There are several lines of evidence to suggest that this is not the case in the VS ribozyme.[131]

An interesting comparison can be made between the deduced structure of the VS ribozyme and the better-understood structure of the hairpin ribozyme. The active sites of both the hairpin and VS ribozymes appear to be formed by the interaction of two loops in a way that brings together a guanine residue and an adenine residue essential for catalysis. In both cases, the guanine residue resides on the strand opposite the scissile phosphate in the same internal loop and the adenine is found in the second loop.[131,133] In the hairpin ribozyme, high-resolution crystal structures show the equivalent G and A residues well positioned to act as the general acid and the base in the reaction (vide supra). Interestingly, though, as shown in

dx.doi.org/10.1021/cr400476k | Chem. Rev. 2014, 114, 4318–4342

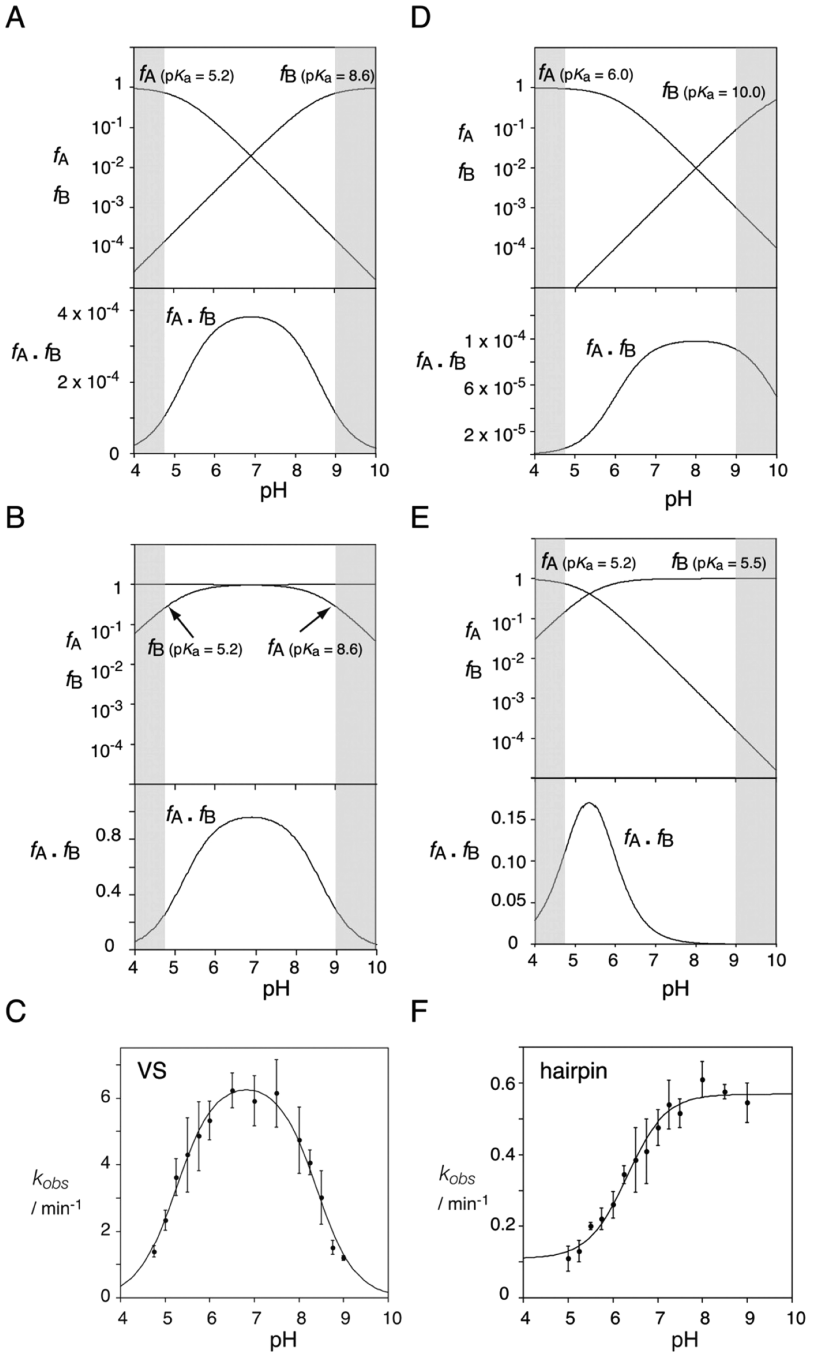

Figure 16. Experimental pH-rate profiles for the VS (C) and hairpin (F) ribozymes and theoretical curves demonstrating the effects of changing magnitude (A,D,E) and identities (A,B) of predicted general acid and base values. Both ribozymes are proposed to have conserved A and G nucleobases that could act as general acid and general base, respectively. Their pH-rate profiles differ significantly, however, indicating different nucleobase roles and the possible modulating influence of a metal ion in the case of the VS ribozyme. Theoretical curves show the influence of changing pKa values on resultant active ribozyme populations. Reprinted with permission from ref 131. Copyright 2011 CSHL Press.

Figure 16, the pH−rate profiles of the HP and VS ribozymes are strikingly different. As discussed, the pH−rate profile of the VS ribozyme is consistent with a role for the conserved A and G acting as general acid and base, respectively, with the stipulation that they exist in specific environments to alter their pK_a values. The pH−rate profile of the hairpin ribozyme, on the other hand, differs significantly in that the activity rises until around pH 6 but does not fall off over the pH range available for ribozyme studies. This indicates that the second ionizable group has a pK_a higher than 9. If the HP and VS ribozymes both use an A at the proton donor, then their active sites create slightly different electronic environments and pK_a values for their conserved adenines. In the case of the conserved G nucleobases, evidence in the case of the HP ribozyme suggests that G8 minimally plays a strong role in positioning and hydrogen bonding around the scissile phosphate and may be ionized in the active site. Current models of the VS ribozyme support ionization of G638, which may play a direct role in proton transfer. As another contrast, unlike the HP ribozyme, the activity of the VS ribozyme is sensitive to identity of

dx.doi.org/10.1021/cr400476k | Chem. Rev. 2014, 114, 4318−4342

supporting metal ion. This has suggested a more direct role for metals in the VS mechanism, although it has been proposed that this role may be mainly to modulate the ionization properties of the nucleobases.[136]

12. GLMS RIBOZYME

The entire field of RNA biology is expanding as new RNA-dependent mechanisms of genetic control are discovered. One of the more fascinating discoveries in this field has been the metabolite-responsive mRNAs.[3,137−139] When metabolites bind the RNA aptamer domain, a particular secondary structure is stabilized that then affects gene expression through either transcription termination or translation initiation.[139] As the switch between the "on" and "off" conformers is dependent on metabolite binding, these RNAs are termed "riboswitches".

In 2004, a new riboswitch was found in a conserved region upstream of the *Bacillus subtilis* GlmS gene that regulates not through a conformational change but through ribozyme activity.[140] Binding of the metabolite glucosamine 6-phosphate (GlcN6P) to this riboswitch results in a site-specific mRNA cleavage reaction, thereby down-regulating expression of the GlcN6P synthetase GlmS ribozyme and further GlcN6P synthesis. The GlmS ribozyme promotes attack by a 2′-OH on its own 3′-phosphodiester bond, making it a class II ribozyme like the HHRz, HP, HDV, and VS ribozymes discussed above, but with a distinct cofactor requirement.

Theoretically, binding of the metabolite could preferentially stabilize an active ribozyme conformation. This is not the case for the GlmS ribozyme, however. Instead, for the GlmS riboswitch/ribozyme, the bound metabolite controls catalysis by actually providing a chemically important functional group for the reaction. The activity of the ribozyme is dependent on the pK_a of the amine of GlcN6P and derivatives thereof.[141,142] Structural studies indicate that, unlike many RNA aptamers, the overall structure of the GlmS ribozyme is independent of metabolite binding[143] but the GlcN6P amine is positioned near the leaving group at the ribozyme active site. Activity studies show that the GlmS ribozyme can achieve high rates of catalysis with a wide range of divalent cations,[140] as well as both millimolar amounts of exchange-inert $Co(NH_3)_6^{3+}$ and molar amounts of K^+.[144] Additionally, active-site phosphorothioate substitutions result in fairly minor inhibition.[144] Taken together, indications from existing biochemical data are that this ribozyme does not depend on inner-sphere metal-ion coordination at the active site for catalysis, but does require dense positive charge, which could provide structural stability.[144]

This indirect role for cations and direct role for the metabolite in the GlmS ribozyme mechanism has been supported by crystal structures of the ribozyme in unbound and inhibitor-bound glucose-6-phosphate and GlcN6P.[145,146] The structure of the GlmS ribozyme with GlcN6P bound indicates that the three nonbridging oxygens of the metabolite phosphate are each bound to at least one of two fully hydrated Mg^{2+} ions (Figure 17). The Mg^{2+} ions, in turn, make outer-sphere contacts with RNA groups, including one RNA nonbridging phosphodiester oxygen. These data support a role for magnesium that is structural, in that the ordered cations both precisely position the cofactor and shield its phosphates from the charge of the RNA backbone. However, it is important to note that the presence of these ions within the active site can also indirectly contribute to catalysis by altering the electrostatic environment of the active site.

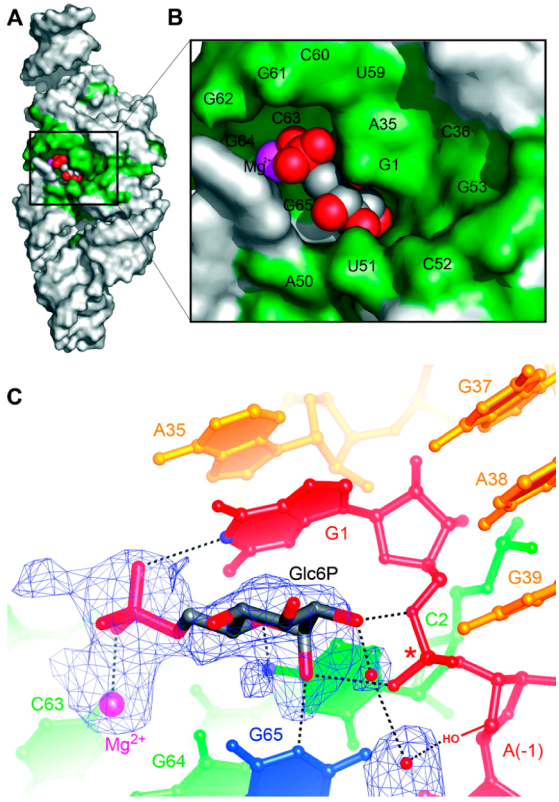

Figure 17. Structure and active site of the GlmS metabolite-sensing ribozyme. (A,B) GlcN6P binds to a cleft in a preformed RNA structure such that (C) its amine can activate ribozyme activity through protonation of the leaving group. A 2′-OH nucleophile is modeled into the deoxy-A(−1) structure. The GlcN6P terminal phosphate is bound to well-ordered Mg^{2+} ions (only one shown here). Reprinted with permission from ref 145. Copyright 2006 AAAS.

A direct measure of the pK_a of the amine group of the GlcN6P cofactor in the GlmS active site, using Raman spectroscopy of the crystallized ribozyme, showed that the amine pK_a is reduced to ∼7.3 within the ribozyme, down ∼0.5 units relative to its value in solution.[147] Results from a solution NMR study found an even larger pK_a reduction of >1 unit upon GlcN6P binding to the GlmS ribozyme.[148] Under normal circumstances, as discussed in previous sections, the negative potential within an RNA would be expected to stabilize protonation and increase the pK_a; this is, in fact, observed for the terminal phosphate of GlcN6P, whose pK_a is increased from 6 to 6.35 within the ribozyme active site.[147] Surprisingly, both GlcN6P pK_a perturbations are ablated for an inactive GlmS ribozyme in which a conserved active-site guanine, G40, is substituted by A. Crystallographic studies do not provide an explanation for this result, instead showing that GlcN6P is bound in the same manner in the G40A mutant,[149] similarly positioned with its amine group available for leaving-group protonation. The only minor change noted in the G40A mutant structure was an increase in apparent hydrogen-bonding distance between the purine at position 40 and the nucleophilic 2′-OH group. Although activation of the 2′-OH nucleophile by G40 could significantly influence catalysis, it is unclear how this might perturb pK_a values of the GlcN6P cofactor located near the leaving group. A greater perturbation than by hydrogen bonding could occur through ionization of G40, but a pK_a analysis of a fluorescent deaza G40 analogue provides no

dx.doi.org/10.1021/cr400476k | *Chem. Rev.* 2014, 114, 4318−4342

evidence for this and instead favors a model in which G40 influences catalysis through hydrogen bonding to the 2′-OH group.[142] It is possible that the metal ions bound to the GlcN6P phosphate in the ribozyme active site contribute to the pK_a of the cofactor, but further work will be necessary to explain their influence and that of G40. Because several nucleolytic ribozymes have conserved guanine nucleobases at the active site, the properties of these conserved guanines including positioning, hydrogen bonding, and ionization are of great interest in the ribozyme field.

13. ARTIFICIAL RIBOZYMES

13.1. Overview

To date, the activities discovered for naturally occurring ribozymes include those shown in Figure 1 of this review. It is evident, however, that RNA in conjunction with metal ions and other cofactors has a vast capacity for selective recognition of small molecules and for tuning of the electronic properties of reactive groups. Not surprisingly, then, there has been great interest in exploring this capacity for substrate binding and reactivity by creating artificial ribozymes.[150] Using the power of in vitro selection to isolate active ribozymes from millions of potential sequences,[151] RNA sequences with a number of different properties have been discovered. There has been great interest in the potential for RNA as a primordial biomolecule and, therefore, in finding RNAs that can catalyze replicative reactions such as an RNA-dependent RNA polymerase[152] that can utilize a two-metal-ion mechanism similar to that described for protein polymerases. An interesting extension to a ribozyme that catalyzes ribozyme synthesis has also been presented.[153] Although the metal-dependent activity of naturally occurring ribozymes has focused on Mg^{2+} as the natural cofactor, RNA certainly binds transition-metal ions,[4,20,21] and in vitro selections for activity can be performed to explore this potential. For example, a Cu-dependent ribozyme that catalyzes phosphate transfer from GTP or thiophosphate transfer from GTPγS has been described, wherein the Cu(II) ion enhances the reaction as a Lewis acid catalyst.[154] As an example of the expanded chemical repertoire available to nucleic acid catalysts, we highlight below just one of the in vitro selected ribozymes, a Diels–Alderase enzyme that has been mechanistically and structurally characterized.

13.2. Diels–Alderase Ribozyme

The RNA world hypothesis suggests that before DNA and protein evolved, early life utilized RNA as both a genetic and catalytic molecule. This hypothesis is one explanation for several key observations, such as RNA's essential role in protein synthesis and the existence of universally conserved nucleotide cofactors.[155,156] A key missing link in the RNA world hypothesis is discovery of catalytic RNAs that are capable of forming carbon–carbon bonds. Seelig and Jäschke used in vitro selection techniques to generate RNA aptamers capable of catalyzing a Diels–Alder cycloaddition reaction, demonstrating that RNA is capable of forming carbon–carbon bonds.[157] This was accomplished by linking an anthracine construct to a randomized pool of candidate 120-nucleotide RNA molecules and reacting the resulting mixture with biotinylated maleimide (Figure 18). Substrates that underwent a Diels–Alder reaction between the anthracine and maleimide resulted in a covalent linkage connecting the catalyzing RNA with the biotin tag. Candidate catalytic RNAs were selected by streptavidin pull-downs followed by reverse transcription and polymerase chain

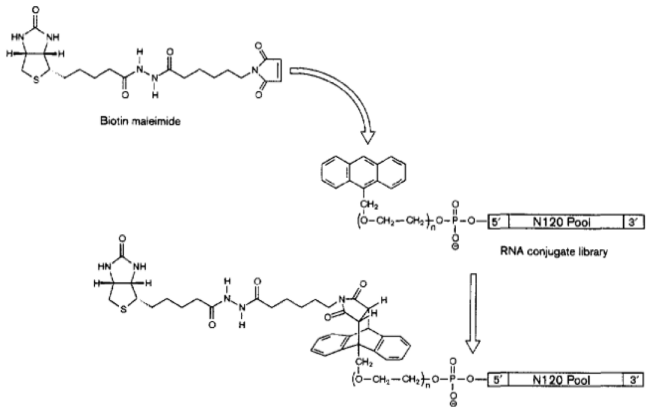

Figure 18. Selection of the Diels–Alderase ribozyme. A biotinylated maleimide was reacted with an anthracine linked to a randomized pool of RNA flanked by priming regions. The products of the reaction resulted in a covalent linkage between the RNA pool and the biotin tag, which was used to separate candidate catalytic RNA sequences. Reprinted with permission from ref 157. Copyright 1999 Elsevier.

reaction (PCR) amplification of the products, and the process was repeated with increasing stringency to further refine the pool. After 10 rounds, the refined library was sequenced, resulting in 42 unique sequences. The best-performing sequence increased the rate of the reaction 18500-fold.

From this pool of sequences, the authors then rationally minimized their structure by truncating one of their candidate ribozymes and removing unpaired regions. The new 49-nucleotide rationally optimized sequence was capable of enhancing the catalytic rate approximately 20000-fold.[157] Although the sequence was selected in 200 mM Na^+ and 100 mM K^+, activity was within 10% when tested under either 300 mM Na^+ or 300 mM K^+, suggesting that the exact identity of monovalent cations is unimportant. The catalytic rate was dependent on Mg^{2+} concentration, however, and reduced by 65% when Mg^{2+} was substituted by Ca^{2+}.[157]

The structure of the 49-mer Diels–Alederase ribozyme was solved in 2005, in both free and product-bound forms (Figure 19).[158,159] It consists of three helices with a nested double pseudoknot junction. Eight Mg^{2+} ions were resolved in this

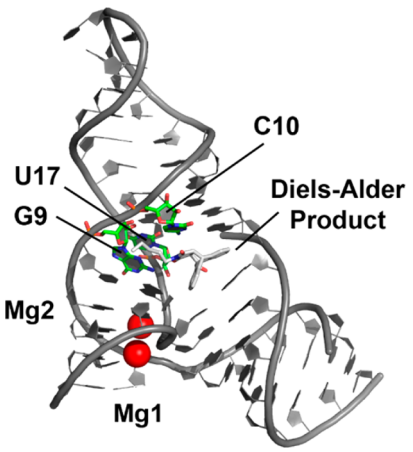

Figure 19. Structure of the Diels–Alderase ribozyme. Mg1 and Mg2, arguably the most important metal ions for maintaining catalytic activity, are shown as red spheres. In green are the three nucleotides involved in important hydrogen bonding, G9, C10, and U17. Figure from PDB 1YKV.

dx.doi.org/10.1021/cr400476k | Chem. Rev. 2014, 114, 4318–4342

structure, two of which appear to mediate interactions between RNA molecules in the crystal lattice, giving six Mg^{2+} ions playing structural roles in the ribozyme. NMR titration experiments suggest that only two of these metal ions are necessary to properly fold the ribozyme.[158] Mg^{2+} ions in sites 1 and 2 appear to be particularly important for forming an active structure, as they interact with a number of nucleotides in close proximity to the active site[158,159] and stabilize the packing of helices 1 and 2 with each other, forming the "bottom" of the active site.[160]

Interestingly, of the six Mg^{2+} ions believed to play a functional role, none were positioned close enough to the binding pocket to directly participate in catalysis.[158] Their role appears to be solely structural. These crystal structures as well as chemical probing experiments[161] suggest that the ribozyme exhibits a preformed active site, as little structural difference is observed in the free and product-bound states. However, recent single-molecule FRET studies suggest that the Diels–Alderase ribozyme undergoes significant structural changes in a Mg^{2+}-dependent manner, fluctuating between an unfolded state, an intermediate state, and a folded state, with the time spent in the folded state dependent on the Mg^{2+} concentration, an observation commonly seen in larger, naturally occurring ribozymes.[162] Kobitski and co-workers suggest that the results seen with single-molecule FRET are consistent with transient opening and closing of the active site, a theory similar to that put forth by Bereźniak and co-workers based on molecular dynamics simulations.[160]

Current understanding of the mechanism of the Diels–Alderase ribozyme suggests that stacking of the anthracine and maleimide is perhaps the most crucial role. For the Diels–Alder reaction to occur, the reactants must be stacked above one another and in parallel, an orientation supported by this ribozyme.[158] This also serves to increase the local concentration of reactants, resulting in a rate increase.

Recent work has shown that several hydrogen bonds play key roles in catalysis. Through careful mutagenesis of the ribozyme, Kraut et al. identified three particularly important hydrogen bonds.[163] The first is located between the 2′-OH of G9 and HN3 of U17. This hydrogen bond supports a key stacking structure running the length of the ribozyme (termed the "spine") and is essential for forming a catalytic ribozyme. Replacement of the interacting partners with a pair of H-bond acceptors completely abolishes ribozyme activity, presumably through disruption of the active-site structure.

The second critical hydrogen bond identified in the Diels–Alderase ribozyme is also structural and occurs between the exocyclic amine of C10 (4-NH_2) and the carbonyl oxygen O2 of U17.[163] This hydrogen bond is an important interstrand interaction that stabilizes the ribozyme and forms the "roof" of the catalytic pocket. Replacing the carbonyl O2 of U17 with an exocyclic amine completely abolishes ribozyme activity. Chemical probing suggests that the ribozyme still folds correctly but the active site takes on a different, inactive structure.

A final set of critical interactions in the Diels–Alderase ribozyme appear to tune reactivity through electron withdrawal at the substrate carbonyl oxygen (Figure 20). This pair of hydrogen bonds occurs between a carbonyl oxygen on the reaction product and both the exocyclic amine of G9 and the 2′-OH of U17.[163] Because this product carbonyl oxygen arises from the maleimide substrate (the dienophile) and it is known that hydrogen bonds to dienophiles can enhance a Diels–Alder

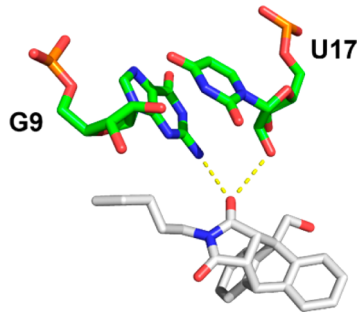

Figure 20. Electronic fine-tuning in the Diels–Alderase ribozyme active site. Two nucleotides (G9 and U17, green) form hydrogen bonds with one of the carbonyl oxygens of the reaction product (gray). The carbonyl oxygen arises from the dienophile in the Diels–Alder reaction. Figure from PDB 1YKV.

reaction,[164] it is believed that this interaction might play a key role in rate enhancement. The authors found that this was the case, although the effect was not as severe as abolishing one of the structural hydrogen bonds discussed above, suggesting that hydrogen-bond-dependent electron withdrawal of the dienophile plays a role but structure of the active site is overall more important. Thus, in the Diels–Alderase ribozyme, the positioning and orientation of substrates plays the major role in catalysis, and fine-tuning through directed hydrogen bonds in the RNA active site also plays a role.

14. DNA-BASED CATALYSTS

With the exception of the ribose 2′-OH group, the functional groups involved in RNA catalysis are also available to DNA. About a decade following the discoveries of RNA catalysis, in 1994, in vitro selection was applied by Breaker and Joyce to achieve the first known DNA catalyst, a Pb^{2+}-dependent phosphodiesterase.[165] To date, no naturally occurring DNA-based enzyme has been discovered, but a rich field of DNA enzymes has been developed through in vitro selection for capabilities that include metal-responsive phosphodiester bond cleavage and ligation, amide bond synthesis, polymerase activity, Diels–Alderase activity, porphyrin metalation, and others.[166−168] There has been an imaginative focus on applications of these catalysts, such as for metal sensors and mechanical transducers. Below, we include a brief description of DNA catalysts with a focus on metal-responsive RNA- and DNA-cleaving DNAzymes and a section on their applications. Recent review articles provide further depth regarding the creative design of in vitro selection approaches and the breadth of DNA catalysts obtained to date.[166−168]

14.1. RNA-Cleaving DNAzymes

The first DNAzyme[165] was discovered through an in vitro selection experiment designed to discover DNA sequences that could cleave a single embedded ribonucleotide in an otherwise DNA target sequence. Selections were performed in the presence of Pb^{2+} to bias the results toward hydrolytic cleavage, as had been previously observed in RNA "leadzymes" that were selected from tRNA-based libraries for Pb^{2+}-dependent cleavage.[169] Subsequently, two main DNAzymes known as "8−17" and "10−23" (numbers based on clones in selection experiments) were characterized that perform cleavage in Mg^{2+}.[170] Figure 21 (upper right) shows the 8−17 DNAzyme, which consists of a characteristic two-arm helical recognition sequence and additional variable stem-loop region. The

dx.doi.org/10.1021/cr400476k | Chem. Rev. 2014, 114, 4318−4342

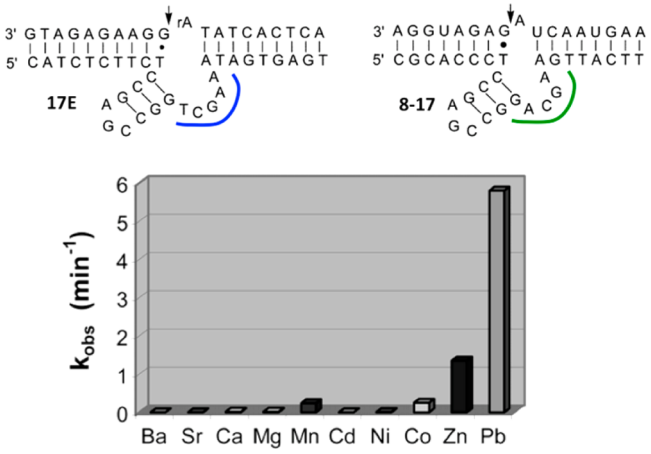

Figure 21. DNAzymes that cleave an embedded ribonucleotide site (vertical arrow). The 17E DNAzyme cleaves selectively in Pb^{2+}, whereas the 8−17 DNAzyme (upper right) is supported by Mg^{2+}. Below, single turnover rate constants of the 17E DNAzyme in the presence of different divalent metal ions at pH 6.0. All metal-ion concentrations were 10 mM, except for that of Pb^{2+}, which was 100 μM. Reprinted with permission from ref 171. Copyright 2003 American Chemical Society.

characteristics of the 8−17 and 10−23 DNAzymes, including likely folding behavior, have been reviewed.[166,171]

RNA-cleaving DNAzymes have been selected for activity in several different metal ions, including Mg^{2+}, Ca^{2+}, Zn^{2+}, Mn^{2+}, Pb^{2+}, and UO_2^{2+} (reviewed in ref 166). There are currently no crystal or NMR structures of an active DNAzyme. It is reasonable to expect that the junction region captures a metal ion that confers selectivity, because metal-dependent variability appears there (for example, the outlined loop in Figure 21).

14.2. DNA-Cleaving DNAzymes

DNA-cleaving DNAzymes have been more elusive than their RNA-cleaving counterparts. The phosphodiester bond in DNA is inherently more stable than that in RNA because of the lack of a proximal 2′-OH nucleophile, and uncatalyzed phosphodiester bond hydrolysis in DNA has a measured half-life in the millions of years.[172] DNA sequences that cleave DNA through nonhydrolytic mechanisms have been discovered; these include oxidative strand cleavage in the presence of Cu(II)/ascorbate[173] and metal-dependent deglycosylation.[174] In 2009, Silverman and co-workers reported isolation of a DNAzyme that cleaved a DNA substrate with a rate enhancement of ~10^{12} in the presence of both Zn^{2+} and Mn^{2+} and demonstrated that the products resulted from hydrolytic chemistry.[175] Further selections in the presence of different metals found a two-nucleotide substitution that produced a DNA-cleaving sequence that required only Zn^{2+}.[176] It was also possible to isolate sequences that were reactive in very low concentrations of lanthanides.[177] The need for Zn^{2+} or lanthanide ions is consistent with a mechanism involving Lewis acid-based properties, such as a deprotonated metal-aqua species and/or activation by metal-ion coordination to the phosphodiester bond.

DNAzyme (and ribozyme) in vitro selections are often performed using a preexisting platform whose design involves capture following cleavage or ligation at a certain sequence. Recently, a selection for DNA-cleaving DNAzymes was performed using a strategy that was designed to find alternative sequences with no preexisting conditions on the target substrate.[178] The strategy involved amplification using a DNA ligase that joins only 5′-phosphate and 3′-OH partners, meaning that the selection discarded hydrolysis catalysts that yielded 3′-phosphates along with other strand-cleavage mechanisms such as oxidation or depurination. Three of the motifs discovered in this selection, which was performed in combined Mg^{2+} and Zn^{2+}, are shown in Figure 22, along with

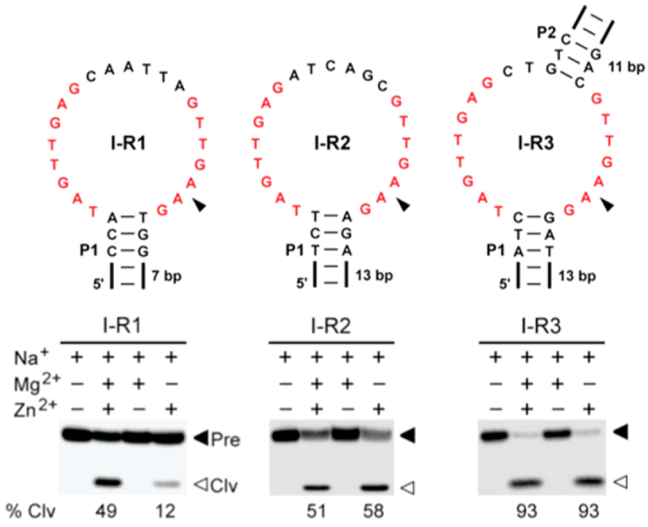

Figure 22. Metal-dependent reactions of DNA-cleaving DNAzymes selected from a general library in the presence of 20 mM Mg^{2+} and 2 mM Zn^{2+}. Reprinted with permission from ref 178. Copyright 2013 American Chemical Society.

their metal-ion dependencies. The selection conditions of 20 mM Mg^{2+} and 2 mM Zn^{2+} are much higher concentrations than expected for intracellular metals. However, two of the selected sequences required only 2 mM Zn^{2+} for activity.

The authors performed genome-wide searches to address the interesting question of whether these self-cleaving sequences occurred naturally and, if so, whether they might be related to genome instability. A handful of naturally occurring sequences were found that contained the 15-nucleotide conserved sequences discovered in one class of the selected DNAzymes (denoted red in Figure 22).[178] Some of these naturally occurring sequences were found to self-cleave slowly in 2 mM Zn^{2+}, but not at a lower value of 50 μM Zn^{2+} that is still high relative to expected intracellular Zn^{2+} concentration. These results suggest that although there are naturally occurring DNA-cleaving sequences that could lead to genome instability, they might not be active under normal intracellular metal concentrations. The authors also demonstrated that their selected DNAzymes could be used in trans configuration to site-specifically cleave a circular M13 bacteriophage genome, pointing to potential biotechnological applications of these and other DNA-cleaving DNAzymes.

14.3. DNAzyme Sensors and Machines

The ion selectivity available in DNAzymes has supported their use as ion-selective sensors.[166] Variants of the 8−17 DNAzyme have been modified with fluorophores and quenchers such that metal-dependent cleavage is detected by an increase in fluorescence as the product strand is released. With these constructs, sensitivities to <10 nM Pb^{2+} [179] and 45 pM UO_2^{2+} [180] have been achieved with high selectivities. Further modifications to enhance brightness with quantum dots and

dx.doi.org/10.1021/cr400476k | Chem. Rev. 2014, 114, 4318−4342

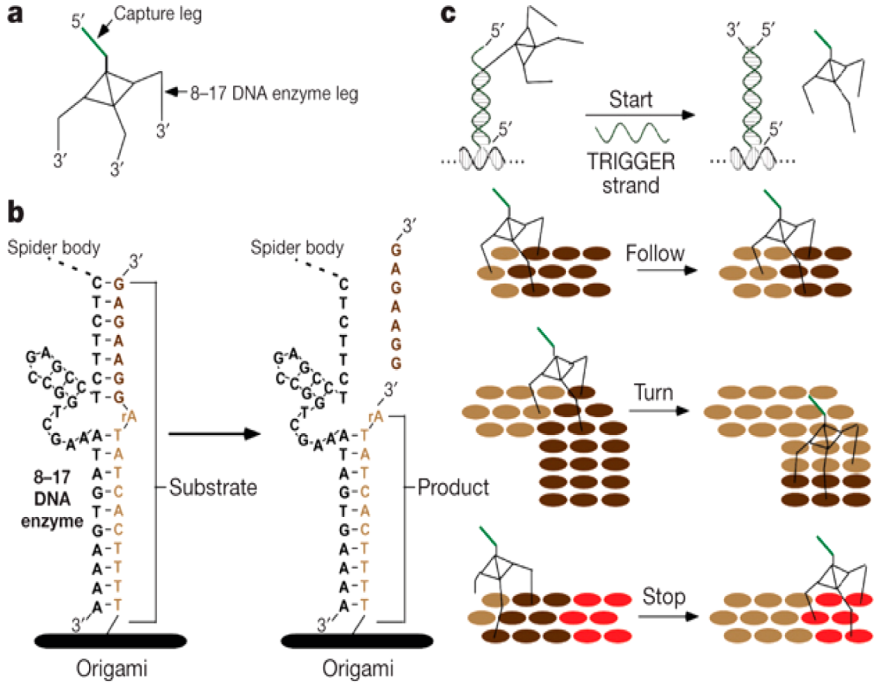

Figure 23. Spider with DNAzyme legs that moves on a surface patterned with substrate oligonucleotides. A DNAzyme spider leg binds and cleaves substrate and is then released from the lower-affinity product helix to reanneal to the next substrate strand. At right, the spider moves through a pattern of low-affinity product (light brown) toward high-affinity substrate (dark brown) strands, stopping at a noncleavable all-deoxy stop (red) oligonucleotide. Reprinted with permission from ref 184. Copyright 2010 Nature Press.

convenience with label-free methods have created practical nucleic-acid-based metal-ion sensors for applications in testing drinking water and other types of contamination.[166]

Among the DNAzyme reactions used for detecting analytes, a second particularly sensitive option is the peroxidase activity catalyzed by a guanine-rich DNA that binds hemin (ferric porphyrin). In the presence of H_2O_2, this DNA hemin aptamer releases hydroxyl radicals[181,182] and can be termed a peroxidase DNAzyme. Coupled with chemiluminescent detection and separated as a two-piece split aptamer that recombines upon hybridization to a particular sequence, this DNAzyme has been used to detect specific DNA and RNA sequences (reviewed in ref 183).

The inherent stability of DNAzymes makes them attractive for other applications that take advantage of changes following substrate cleavage. For example, RNA-cleaving 8−17 DNAzymes have been used as the legs of DNA "spiders" that act as molecular robots by moving along a DNA landscape that is patterned with substrate strand sequences (Figure 23).[184] When a DNAzyme leg cleaves a substrate strand (in the presence of Zn^{2+}), the leg is "released" from the shorter product strand and will anneal to the next available full substrate. This results in net directional movement of about 3 nm per minute under the experimental conditions and total distances of up to 100 nm.[184]

15. CONCLUDING REMARKS

RNA-assisted catalysis by ribozymes plays select but critical roles in nature. Despite seemingly restricted diversity in chemical properties, the sequence and structural diversity available to RNA supports selective positioning of reactants and metal-ion and other cofactors, along with providing general acid and base properties and fine-tuning of environmental pK_a values. Early concepts of RNA as a scaffold for Mg^{2+}-ion catalysts have evolved to a continuum of metal-ion participation in RNA catalysis, with active sites showing a range of interactions that span an absence of direct metal-ion interactions to precisely positioned clusters of three or more specific cations. New frontiers in this area include the influence and feedback between metal-ion homeostasis and cellular metal concentrations on RNA structure and function, and the regional electrostatic effects of bound metals at catalytic sites. DNA-based catalysts, although not yet found in nature, show potential for myriad reactions including metal-dependent RNA and DNA cleavage, and their applications as metal sensors and mechanical machines have been demonstrated. In the context of the vast counterion atmosphere supported by nucleic acids and the potential nonspecific reactivity of metal ions in backbone hydrolysis, it is amazing that RNAs have evolved to selectively harness metal ions for function and that naturally occurring sequences of both RNA and DNA have evaded unwanted reactivities.

AUTHOR INFORMATION

Corresponding Author

*E-mail: derose@uoregon.edu.

Present Address

[§]Department of Cellular and Molecular Biology, University of Texas-Austin, Austin, TX 78712-0159.

Notes

The authors declare no competing financial interest.

Biographies

Luke Ward received his Bachelor's degree at the University of Missouri, Columbia. He did his doctoral research in the DeRose laboratory at the University of Oregon and received his Ph.D. in 2012. He is currently working as a postdoctoral researcher in the Russell laboratory at the University of Texas at Austin. Generally interested in RNA structural biology, he is currently focusing on single-molecule characterization of RNA chaperone activity.

Kory Plakos received his B.S. in Biochemistry from the University of California, Santa Barbara (UCSB), in 2007. After graduation, he worked in the Tom Soh laboratory at UCSB for two years developing DNA aptamer-based biosensors. Kory is currently working toward his Ph.D. in the DeRose laboratory at the University of Oregon. He is generally interested in high-throughput structure determination of complex RNAs, with a focus on structure–function relationships.

Victoria DeRose is currently Professor of Chemistry and Biochemistry at the University of Oregon. She obtained a Bachelor's degree in Chemistry from the University of Chicago, where she spent time in the laboratory of Robert Haselkorn studying the molecular biology of nitrogen fixation in cyanobacteria. She joined the laboratories of Ken Sauer and Mel Klein as a Ph.D. student at the University of California-Berkeley, working on spectroscopic studies of the tetranuclear Mn cluster catalyzing oxygen evolution in PSII. As a postdoctoral researcher in the laboratory of Brian Hoffman at Northwestern University, she applied "advanced EPR techniques" to problems in metalloenzymes including nitrogenase and methane monooxygenase. She began as an Assistant Professor at Texas A&M University in 1995, where she sought to develop a program investigating the metallobiochemistry of RNA and ribozymes, with an emphasis on spectroscopic methods. She was promoted to Associate Professor in 2001, and in 2006, she moved to the University of Oregon. She is generally interested in the interface of chemistry and biology, with an emphasis on bioinorganic and biophysical properties of proteins and nucleic acids.

ACKNOWLEDGMENTS

Work in the DeRose laboratory on the influence of metal ions on RNA structure and catalysis was funded by the NSF (Grants CHE1153147 and CHE0111696) and the NIH (Grant GM058096). L.W. and K.P. were supported by NIH T32 Grant GM007759-29. L.W. was also supported by the NSF GK-12 program (Grant DGE-0742540). We thank members of the DeRose laboratory for helpful discussions.

REFERENCES

(1) *The RNA World*, 3rd ed.; Gesteland, R.F., Cech, T.R., Atkins, J.F., Eds.; Cold Spring Harbor Laboratory (CSHL) Press: Cold Spring Harbor, NY, 2013.
(2) DeRose, V. J. *Chem. Biol.* **2002**, *9*, 961–969.
(3) Ferre-D'Amare, A.; Winkler, W. C. *Met. Ions Life Sci.* **2011**, *9*, 141.
(4) Hsiao, C.; Chou, I.-C.; Okafor, C. D.; Bowman, J. C.; O'Neill, E. B.; Athavale, S. S.; Petrov, A. S.; Hud, N. V.; Wartell, R. M.; Harvey, S. C.; Williams, L. D. *Nat. Chem.* **2013**, *5*, 525.
(5) Pyle, A. M. *Science* **1993**, *261*, 709.
(6) Steitz, T. A.; Steitz, J. A. *Proc. Natl. Acad. Sci. U.S.A.* **1993**, *90*, 6498.
(7) Wilcox, J. L.; Ahluwalia, A. K.; Bevilacqua, P. C. *Acc. Chem. Res.* **2011**, *44*, 1270.
(8) Golden, B. L. *Biochemistry* **2011**, *50*, 9424.
(9) Sigel, R. K. O.; Pyle, A. M. *Chem. Rev.* **2007**, *107*, 97.
(10) Ma, J.; Haldar, S.; Khan, M. A.; Sharma, S. D.; Merrick, W. C.; Theil, E. C.; Gross, D. J. *Proc. Natl. Acad. Sci. U.S.A.* **2012**, *109*, 8417.
(11) (a) Rodnina, M. V.; Beringer, M.; Wintermeyer, W. *Trends Biochem. Sci.* **2007**, *32*, 20. (b) Leung, E. K.; Suslov, N.; Tuttle, N.; Sengupta, R.; Piccirilli, J. A. *Annu. Rev. Biochem.* **2011**, *80*, 527.
(12) Fedor, M. J. *Annu. Rev. Biophys.* **2009**, *38*, 271.
(13) Schnabl, J.; Sigel, R. K. O. *Curr. Opin. Chem. Biol.* **2010**, *14*, 269.
(14) *Ribozymes and RNA Catalysis*; Lilley, D. M. J., Eckstein, F., Eds.; Royal Society of Chemistry: Cambridge, U.K., 2008.
(15) Draper, D. E.; D. Grilley, D.; Soto, A. M. *Annu. Rev. Biophys. Biomol. Struct.* **2005**, *34*, 221.
(16) Frederiksen, J. K.; Piccirilli, J. A. *Methods* **2009**, *49*, 148.
(17) DeRose, V. J. Characterization of nucleic acid metal ion binding by spectroscopic techniques. In *Metal Ion Interactions with Nucleic Acids*; Hud, N., Ed.; RSC Publishing: Cambridge, U.K., 2008; pp 154–175.
(18) Hunsicker-Wang, L. M.; Vogt, M.; DeRose, V. J. EPR Methods to Study Specific Metal-Ion Binding Sites in RNA In *Methods in Enzymology*; Herschlag, D., Ed.; Academic Press: New York, 2009; Vol. *468*, pp 335–368.
(19) Chu, V. G.; Bai, Y.; Lipfert, J.; Herschlag, D.; Doniach, S. *Curr. Opin. Chem. Biol.* **2008**, *12*, 619.

(20) DeRose, V. J.; Burns, S.; Vogt, M.; Kim, N.-K. RNA and DNA as Ligands. In *Comprehensive Coordination Chemistry II*; McCleverty, J. A., Meyers, T. J., Eds.; Elsevier: Oxford, U.K., 2003; pp 787−813.
(21) Freisinger, E.; Sigel, R. K. O. *Coord. Chem. Rev.* **2007**, *251*, 1834.
(22) Narlikar, G. J.; Herschlag, D. *Annu. Rev. Biochem.* **1997**, *66*, 19.
(23) Butcher, S. E.; Pyle, A. M. *Acc. Chem. Res.* **2011**, *44*, 1302.
(24) Uhlenbeck, O. C. *Biopolymers* **2009**, *91*, 811.
(25) Lilley, D. M. J. *Nat. Struct. Biol.* **2003**, *10*, 672.
(26) Ora, M.; Lönnberg, T.; Lönnberg, H. Thio Effects as a Tool for Mechanistic Studies of the Cleavage of RNA Phosphodiester Bonds: The Chemical Basis. In *From Nucleic Acids Sequences to Molecular Medicine*; Erdmann, V. A., Barciszewski, J., Eds.; RNA Technologies Series; Springer Verlag: Berlin, 2012; pp 47−66.
(27) Li, N.-S.; Frederiksen, J. K.; Piccirilli, J. A. *Acc. Chem. Res.* **2011**, *44*, 1257.
(28) McDowell, S. E.; Spackova, N.; Sponer, J.; Walter, N. G. *Biopolymers* **2007**, *85*, 169.
(29) Wong, K.-Y.; Gu, H.; Zhang, S.; Piccirilli, J. A.; Harris, M. E.; York, D. M. *Angew. Chem., Int. Ed.* **2012**, *51*, 647.
(30) Bida, J. P.; Das, R. *Curr. Opin. Struct. Biol.* **2012**, *22*, 457−466.
(31) Veeraraghavan, N.; Ganguly, A.; Golden, B. L.; Bevilacqua, P. C.; Hammes-Schiffer, S. *J. Phys. Chem. B* **2011**, *115*, 8346.
(32) Kruger, K.; Grabowski, P. J.; Zaug, A. J.; Sands, J.; Gottschling, D. E.; Cech, T. R. *Cell* **1982**, *31*, 147.
(33) Haugen, P.; Simon, D. M.; Bhattacharya, D. *Trends Genet.* **2005**, *21*, 111.
(34) Stahley, M.; Strobel, S. *Curr. Opin. Struct. Biol.* **2006**, *16*, 319.
(35) Woodson, S. A. *Curr. Opin. Struct. Biol.* **2005**, *15*, 324.
(36) Stahley, M.; Adams, P.; Wang, J.; Strobel, S. *J. Mol. Biol.* **2007**, *372*, 89.
(37) Sengupta, R. N.; Herschlag, D.; Piccirilli, J. A. *ACS Chem. Biol.* **2012**, *7*, 294.
(38) Adams, P. L.; Stahley, M. R.; Gill, M. L.; Kosek, A. B.; Wang, J.; Strobel, S. A. *RNA* **2004**, *10*, 1867.
(39) Golden, B. L.; Kim, H.; Chase, E. *Nat. Struct. Mol. Biol.* **2005**, *12*, 82.
(40) Guo, F.; Gooding, A. R.; Cech, T. R. *Mol. Cell* **2004**, *16*, 351.
(41) Stahley, M. R.; Strobel, S. A. *Science* **2005**, *309*, 1587.
(42) Eskes, R.; Liu, L.; Ma, H. W.; Chao, M. Y.; Dickson, L.; Lambowitz, A. M.; Perlman, P. S. *Mol. Cell. Biol.* **2000**, 8432.
(43) Guo, H. T.; Karberg, M.; Long, M.; Jones, J. P.; Sullenger, B.; Lambowitz, A. M. *Science* **2000**, 452.
(44) Matsuura, M.; Saldanha, R.; Ma, H. W.; Wank, H.; Yang, J.; Mohr, G.; Cavanagh, S.; Dunny, G. M.; Belfort, M.; Lambowitz, A. M. *Genes Dev.* **1997**, 2910.
(45) Marcia, M.; Pyle, A. M. *Cell* **2012**, *151*, 497.
(46) Sigel, R. *Eur. J. Inorg. Chem.* **2005**, 2281.
(47) Erat, M. C.; Zerbe, O.; Fox, T.; Sigel, R. *ChemBioChem* **2007**, 306.
(48) Podar, M.; Perlman, P. S.; Padgett, R. A. *Mol. Cell. Biol.* **1995**, *15*, 4466.
(49) Padgett, R. A.; Podar, M.; Boulanger, S. C.; Perlman, P. S. *Science* **1994**, *266*, 1685.
(50) Gordon, P. M.; Sontheimer, E. J.; Piccirilli, J. A. *Biochemistry* **2000**, 12939.
(51) Gordon, P. M.; Sontheimer, E. J.; Piccirilli, J. A. *RNA* **2000**, 199.
(52) Gordon, P. M.; Fong, R.; Piccirilli, J. A. *Chem. Biol.* **2007**, 607.
(53) Toor, N.; Keating, K.; Taylor, S.; Pyle, A. *Science* **2008**, *320*, 77.
(54) Gregan, J.; Kolisek, M.; Schweyen, R. J. *Genes Dev.* **2001**, *15*, 2229.
(55) Chalamcharla, V. R.; Curcio, M. J.; Belfort, M. *Genes Dev.* **2010**, *24*, 827.
(56) Truong, D. M.; Sidote, D. J.; Russell, R.; Lambowitz, A. M. *Proc. Natl. Acad. Sci. U.S.A.* **2013**, *110*, E3800.
(57) Mondragon, A. *Annu. Rev. Biophys.* **2013**, *42*, 537.
(58) Guerriertakada, C.; Gardiner, K.; Marsh, T.; Pace, N.; Altman, S. *Cell* **1983**, *35*, 849.
(59) Holzmann, J.; Frank, P.; Loffler, E.; Bennett, K. L.; Gerner, C.; Rossmanith, W. *Cell* **2008**, *135*, 462.
(60) Howard, M. J.; Lim, W. H.; Fierke, C. A.; Koutmos, M. *Proc. Natl. Acad. Sci. U.S.A.* **2012**, *109*, 16149.
(61) Thomas, B. C.; Li, X.; Gegenheimer, P. *RNA* **2000**, *6*, 545.
(62) Torres-Larios, A.; Swinger, K. K.; Krasilnikov, A. S.; Pan, T.; Mondragon, A. *Nature* **2005**, 584.
(63) Kazantsev, A. V.; Krivenko, A. A.; Harrington, D. J.; Holbrook, S. R.; Adams, P. D.; Pace, N. R. *Proc. Natl. Acad. Sci. U.S.A.* **2005**, *102*, 13392.
(64) Altman, S. *Mol. BioSyst.* **2007**, *3*, 604.
(65) Kirsebom, L. *Biochimie* **2007**, *89*, 1183.
(66) Smith, J. K.; Hsieh, J.; Fierke, C. A. *Biopolymers* **2007**, *87*, 329.
(67) Beebe, J. A.; Kurz, J. C.; Fierke, C. A. *Biochemistry* **1996**, 10493.
(68) Pan, T. *Biochemistry* **1995**, *34*, 902.
(69) Brannvall, M.; Mikkelsen, N. E.; Kirsebom, L. A. *Nucleic Acids Res.* **2011**, 1426.
(70) Brannvall, M.; Kirsebom, L. A. *Proc. Natl. Acad. Sci. U.S.A.* **2001**, 12943.
(71) Kikovska, E.; Mikkelsen, N. E.; Kirsebom, L. A. *Nucleic Acids Res.* **2005**, *33*, 6920.
(72) Smith, D.; Pace, N. R. *Biochemistry* **1993**, *32*, 3273.
(73) Chen, Y.; Li, X. Q.; Gegenheimer, P. *Biochemistry* **1997**, *36*, 2425.
(74) Pfeiffer, T.; Tekos, A.; Warnecke, J. M.; Drainas, D.; Engelke, D. R.; Seraphin, B.; Hartmann, R. K. *J. Mol. Biol.* **2000**, *298*, 559.
(75) Thomas, B. C.; Chamberlain, J.; Engelke, D. R.; Gegenheimer, P. *RNA* **2000**, *6*, 554.
(76) Warnecke, J. M.; Held, R.; Busch, S.; Hartmann, R. K. *J. Mol. Biol.* **1999**, *290*, 433.
(77) Warnecke, J. M.; Sontheimer, E. J.; Piccirilli, J. A.; Hartmann, R. K. *Nucleic Acids Res.* **2000**, *28*, 720.
(78) Brannvall, M.; Kikovska, E.; Kirsebom, L. A. *Nucleic Acids Res.* **2004**, *32*, 5418.
(79) Sun, L.; Harris, M. E. *RNA* **2007**, *13*, 1505.
(80) Cassano, A. G.; Anderson, V. E.; Harris, M. E. *Biochemistry* **2004**, *43*, 10547.
(81) Reiter, N. J.; Osterman, A.; Torres-Larios, A.; Swinger, K. K.; Pan, T.; Mondragon, A. *Nature* **2010**, *468*, 784.
(82) Kazantsev, A. V.; Krivenko, A. A.; Harrington, D. J.; Holbrook, S. J.; Adams, P. D.; Pace, N. R. *Proc. Natl. Acad. Sci. U.S.A.* **2005**, *102*, 13392.
(83) Lai, M. M. *Annu. Rev. Biochem.* **1995**, *64*, 259.
(84) Salehi-Ashtiani, K.; Lupták, A.; Litovchick, A.; Szostak, J. W. *Science* **2006**, *313*, 1788.
(85) Webb, C.-H. T.; Luptak, A. *RNA Biol.* **2011**, *8*, 719.
(86) Ferre-D'Amare, A. R.; Zhou, K. H.; Doudna, J. A. *Nature* **1998**, *395*, 567.
(87) Luptak, A.; Ferre-D'Amare, A. R.; Zhou, K. H.; Zilm, K. W.; Doudna, J. A. *J. Am. Chem. Soc.* **2001**, *123*, 8447.
(88) Gong, B.; Chen, J.-H.; Chase, E.; Chadalavada, D. M.; Yajima, R.; Golden, B. L.; Bevilacqua, P. C.; Carey, P. R. *J. Am. Chem. Soc.* **2007**, *129*, 13335.
(89) Ke, A.; Zhou, K.; Ding, F.; Cate, J. H. D.; Doudna, J. A. *Nature* **2004**, *429*, 201.
(90) Perrotta, A. T.; Shih, I.; Been, M. D. *Science* **1999**, *286*, 123.
(91) Das, S. R.; Piccirilli, J. A. *Nat. Chem. Biol.* **2008**, *1*, 45.
(92) Golden, B. L.; Hammes-Schiffer, S.; Carey, P. R.; Bevilacqua, P. C. An integrated picture of HDV ribozyme catalysis. In *Biophysics of RNA Folding*. Springer: New York, 2013; 135−168.
(93) Nakano, S.; Chadalavada, D. M.; Bevilacqua, P. C. *Science* **2000**, *287*, 1493.
(94) Nakano, S.; Proctor, D. J.; Bevilacqua, P. C. *Biochemistry* **2001**, *40*, 12022.
(95) Chen, J.-H.; Yajima, R.; Chadalavada, D. M.; Chase, E.; Bevilacqua, P. C.; Golden, B. L. *Biochemistry* **2010**, *49*, 6508.
(96) Veeraraghavan, N.; Ganguly, A.; Chen, J.; Bevilacqua, P. C.; Hammes-Schiffer, S.; Golden, B. L. *Biochemistry* **2011**, *50*, 2672.
(97) Fauzi, H.; Kawakami, J.; Nishikawa, F.; Nishikawa, S. *Nucleic Acids Res.* **1997**, *25*, 3124.

(98) Ganguly, A.; Bevilacqua, P. C.; Hammes-Schiffer, S. *J. Phys. Chem. Let.* **2011**, *2*, 2906.
(99) Chen, J.; Ganguly, A.; Miswan, Z.; Hammes-Schiffer, S.; Bevilacqua, P. C.; Golden, B. L. *Biochemistry* **2013**, *52*, 557.
(100) Hutchins, C. J.; Rathjen, P. D.; Forster, A. C.; Symons, R. H. *Nucleic Acids Res.* **1986**, 3627.
(101) Hammann, C.; Luptak, A.; Perrealt, J.; de la Pena, M. *RNA* **2012**, *18*, 871.
(102) Martick, M.; Horan, L.; Noller, H.; Scott, W. *Nature* **2008**, 5.
(103) Blount, K. E.; Uhlenbeck, O. C. *Annu. Rev. Biophys. Biomol. Struct.* **2005**, 415.
(104) Khvorova, A.; Lescoute, A.; Westhof, E.; Jayasena, S. D. *Nat. Struct. Biol.* **2003**, *10*, 872.
(105) Osborne, E.; Schaak, J.; DeRose, V. J. *RNA* **2005**, *11*, 187.
(106) O'Rear, J. L.; Wang, S.; Feig, A. L.; Beigelman, L.; Uhlenbeck, O. C.; Herschlag, D. *RNA* **2001**, *7*, 537.
(107) Boots, J. L.; Canny, M. D.; Azimi, E.; Pardi, A. *RNA* **2008**, *14*, 2212.
(108) Hunsicker, L. M.; DeRose, V. J. *J. Inorg. Biochem.* **2000**, *80*, 271.
(109) Wang, S. L.; Karbstein, K.; Peracchi, A.; Beigelman, L.; Herschlag, D. *Biochemistry* **1999**, 14363.
(110) Ward, W. L.; DeRose, V. J. *RNA* **2012**, *18*, 16.
(111) Martick, M.; Scott, W. *Cell* **2006**, *126*, 309.
(112) Martick, M.; Lee, T.-S.; York, D. M.; Scott, W. G. *Chem. Biol.* **2008**, *15*, 332.
(113) Thomas, J. M.; Perrin, D. M. *J. Am. Chem. Soc.* **2008**, *130*, 15467.
(114) Roychowdhury-Saha, M.; Burke, D. *RNA* **2006**, *12*, 1846.
(115) Osborne, E. M.; Ward, W. L.; Ruehle, M.; DeRose, V. J. *Biochemistry* **2009**, *48*, 10654.
(116) Lee, T.; Lopez, C. S.; Giambasu, G. M.; Martick, M.; Scott, W. G.; York, D. M. J. *J. Am. Chem. Soc.* **2008**, 3053.
(117) Ferre-D'Amare, A. R. *Biopolymers* **2004**, *73*, 71.
(118) Fedor, M. J. *J. Mol. Biol.* **2000**, *297*, 269.
(119) Kuzmin, Y. I.; Da Costa, C. P.; Cottrell, J. W.; Fedor, M. J. *J. Mol. Biol.* **2005**, *349*, 989.
(120) Cottrell, J. W.; Scott, L. G.; Fedor, M. J. *J. Biol. Chem.* **2011**, *286*, 17658.
(121) Liberman, J. A.; Guo, M.; Jenkins, J. L.; Krucinska, J.; Chen, Y. Y.; Carey, P. R.; Wedekind, J. E. *J. Am. Chem. Soc.* **2012**, *134*, 16933.
(122) Guo, H. C.; Collins, R. *EMBO J.* **1995**, *14*, 368.
(123) Kennell, J. C.; Saville, B. J.; Mohr, S.; Kuiper, M. T.; Sabourin, J. R.; Collins, R. A.; Lambowitz, A. M. *Gene. Dev.* **1995**, *9*, 294.
(124) Lilley, D. M. J. *RNA* **2004**, *10*, 151.
(125) Beattie, T.; Olive, J.; Collins, R. *Proc. Natl. Acad. Sci. U.S.A.* **1995**, *92*, 4686.
(126) Lafontaine, D. A.; Norman, D. G.; Lilley, D. M. J. *EMBO J.* **2002**, *21*, 2461.
(127) Lafontaine, D. A.; Wilson, T. J.; Zhao, Z.-Y.; Lilley, D. M. J. *J. Mol. Biol.* **2002**, *323*, 23.
(128) Rastogi, T.; Beattie, T. L.; Olive, J. E.; Collins, R. *EMBO J.* **1996**, *15*, 2820.
(129) Desjardins, G.; Bonneau, E.; Girard, N.; Boisbouvier, J.; Legault, P. *Nucleic Acids Res.* **2011**, *39*, 4427.
(130) Sood, V. D.; Beattie, T. L.; Collins, R. A. *J. Mol. Biol.* **1998**, *282*, 741.
(131) Wilson, T. J.; Lilley, D. M. J. *RNA* **2011**, *17*, 213.
(132) Hiley, S.; Sood, V.; Fan, J.; Collins, R. *EMBO J.* **2002**, *21*, 4691.
(133) Wilson, T. J.; McLeod, A. C.; Lilley, D. M. J. *EMBO J.* **2007**, *26*, 2489.
(134) Wilson, T. J.; Li, N.-S.; Lu, J.; Frederiksen, J. K.; Piccirilli, J. A.; Lilley, D. M. J. *Proc. Natl. Acad. Sci. U.S.A.* **2010**, *107*, 11751.
(135) Smith, M. D.; Collins, R. A. *Proc. Natl. Acad. Sci. U.S.A.* **2007**, *104*, 5818.
(136) Smith, M. D.; Mehdizadeh, R.; Olive, J. E.; Collins, R. A. *RNA* **2008**, *14*, 1942.
(137) Mironov, A. S.; Gusarov, I.; Rafikov, R.; Lopez, L. E.; Shatalin, K.; Kreneva, R. A.; Perumov, D. A.; Nudler, E. *Cell* **2002**, *111*, 747.
(138) Winkler, W. C.; Cohen-Chalamish, S.; Breaker, R. R. *Proc. Natl. Acad. Sci. U.S.A.* **2002**, *99*, 15908.
(139) Winkler, W. C.; Breaker, R. R. *ChemBioChem* **2003**, *4*, 1024.
(140) Winkler, W.; Nahvi, A.; Roth, A.; Collins, J.; Breaker, R. *Nature* **2004**, *428*, 281.
(141) McCarthy, T. J.; Plog, M. A.; Floy, S. A.; Jansen, J. A.; Soukup, J K.; Soukup, G. A. *Chem. Biol.* **2005**, *12*, 1221.
(142) Viladoms, J.; Scott, L. G.; Fedor, M. J. *J. Am. Chem. Soc.* **2011**, *133*, 18388.
(143) Hampel, K. J.; Tinsley, M. M. *Biochemistry* **2006**, *45*, 7861.
(144) Roth, A.; Nahvi, A.; Lee, M.; Jona, I.; Breaker, R. R. *RNA* **2006**, *12*, 607.
(145) Klein, D. J.; Ferre-D'Amare, A. R. *Science* **2006**, *313*, 1752.
(146) Cochrane, J. C.; Lipchock, S. V.; Strobel, S. A. *Chem. Biol.* **2007**, *14*, 95.
(147) Gong, B.; Klein, D. J.; Ferré-D'Amaré, A. R; Carey, P. R. *J. Am. Chem. Soc.* **2011**, *133*, 14188.
(148) Davis, J. H.; Dunican, B. F.; Strobel, S. A. *Biochemistry* **2011**, *50*, 7236.
(149) Klein, D. J.; Been, M. D.; Ferre-D'amare, A. R. *J. Am. Chem. Soc.* **2007**, *129*, 14858.
(150) Jaschke, A. *Curr. Opin. Struct. Biol.* **2001**, *11*, 321.
(151) Yarus, M. *Science* **2011**, *332*, 181.
(152) Shechner, D. M.; Grant, R. A.; Bagby, S. C.; Koldobskaya, Y.; Piccirilli, J. A.; Bartel, D. P. *Science* **2009**, *326*, 1271.
(153) Wochner, A.; Attwater, J.; Coulson, A.; Holliger, P. *Science* **2011**, *332*, 209.
(154) Biondi, E.; Poudyal, R. R.; Forgy, J. C.; Sawyer, A. W.; Maxwell, A. W. R.; Burke, D. H. *Nucleic Acids Res.* **2013**, *41*, 3327.
(155) Müller, U. *Cell. Mol. Life Sci.* **2006**, *63*, 961.
(156) Neveu, M.; Kim, H.-J.; Benner, S. A. *Astrobiology* **2013**, *13*, 391.
(157) Seelig, B.; Jäschke, A. *Chem. Biol.* **1999**, *6*, 167.
(158) Serganov, A.; Keiper, S.; Malinina, L.; Tereshko, V.; Skripkin, E.; Höbartner, C.; Polonskaia, A.; Phan, A. T.; Wombacher, R.; Micura, R.; Dauter, Z.; Jäschke, A.; Patel, D. J. *Nat. Struct. Mol. Biol.* **2005**, *12*, 218.
(159) Wedekind, J. E. *Met. Ions Life Sci.* **2011**, *9*, 299.
(160) Bereźniak, T.; Zahran, M.; Imhof, P.; Jäschke, A.; Smith, J. C. *J. Am. Chem. Soc.* **2010**, *132*, 12587.
(161) Keiper, S.; Bebenroth, D.; Seelig, B.; Westhof, E.; Jäschke, A. *Chem. Biol.* **2004**, *11*, 1217.
(162) Kobitski, A. Y.; Nierth, A.; Helm, M.; Jäschke, A.; Nienhaus, G. U. *Nucleic Acids Res.* **2007**, *35*, 2047.
(163) Kraut, S.; Bebenroth, D.; Nierth, A.; Kobitski, A. Y.; Nienhaus, G. U.; Jäschke, A. *Nucleic Acids Res.* **2012**, *40*, 1318.
(164) Woodward, R.; Hoffmann, R. *Angew. Chem., Int. Ed.* **1969**, *8*, 781.
(165) Breaker, R. R.; Joyce, G. F. *Chem. Biol.* **1994**, *1*, 223.
(166) Lan, T.; Lu, Y. Metal Ion-Dependent DNAzymes and Their Applications as Biosensors. In *Metal Ions in Life Sciences*; Springer: New York, 2012; Vol. *10*, Chapter 8, pp 217−248.
(167) Silverman, S. K. *Angew. Chem., Int. Ed.* **2010**, *49*, 7180.
(168) Schlosser, K.; Li, Y. *Chem. Biol.* **2009**, *16*, 311.
(169) Pan, T.; Uhlenbeck, O. C. *Nature* **1992**, *358*, 560.
(170) Santoro, S. W.; Joyce, G. F. *Proc. Natl. Acad. Sci. U.S.A.* **1997**, *94*, 4262.
(171) Brown, A. K.; Li, J.; Pavot, C. M-B.; Lu, Y. *Biochemistry* **2003**, *42*, 7152.
(172) Schroeder, G. K.; Lad, C.; Wyman, P.; Williams, N. H.; Wolfenden, R. *Proc. Natl. Acad. Sci. U.S.A.* **2006**, *103*, 4052.
(173) Carmi, N.; Shultz, L. A.; Breaker, R. R. *Chem. Biol.* **1996**, *3*, 1039.
(174) Sheppard, T. L.; Ordoukhanian, P.; Joyce, G. F. *Proc. Natl. Acad. Sci. U.S.A.* **2000**, *97*, 7802.
(175) Chandra, M.; Sachdeva, A.; Silverman, S. K. *Nat. Chem. Biol.* **2009**, *5*, 718.
(176) Xiao, Y.; Allen, E. R.; Silverman, S. K. *Chem. Commun.* **2011**, *47*, 1749.

(177) Dokukin, V.; Silverman, S. K. *Chem. Sci.* **2012**, *3*, 1707.
(178) Gu, H.; Furukawa, K.; Weinberg, Z.; Berenson, D. F.; Breaker, R. R. *J. Am. Chem. Soc.* **2013**, *135*, 9121.
(179) Li, J.; Lu, Y. *J. Am. Chem. Soc.* **2000**, *122*, 10466.
(180) Liu, J.; Brown, A. K.; Meng, X.; Cropek, D. M.; Istok, J. D.; Watson, D. B.; Lu, Y. *Proc. Natl. Acad. Sci. U.S.A.* **2007**, *104*, 2056.
(181) Travascio, P.; Witting, P. K.; Mauk, A. G.; Sen, D. *J. Am. Chem. Soc.* **2001**, *123*, 1337.
(182) Travascio, P.; Li, Y.; Sen, D. *Chem. Biol.* **1998**, *5*, 505.
(183) Willner, I.; Shlyahovsky, B.; Zayats, M.; Willner, B. *Chem. Soc. Rev.* **2008**, *37*, 1153.
(184) Lund, K.; Manzo, A. J.; Dabby, N.; Michelotti, N.; Johnson-Buck, A.; Nangreave, J.; Taylor, S.; Pei, R.; Stojanovic, M. N.; Walter, N. G.; Winfree, E.; Yan, H. *Nature* **2010**, *465*, 206.